



Search for top squarks in final states with two top quarks and several light-flavor jets in proton-proton collisions at $\sqrt{s} = 13$ TeV

The CMS Collaboration*

Abstract

Many new physics models, including versions of supersymmetry characterized by R -parity violation (RPV), compressed mass spectra, long decay chains, or additional hidden sectors, predict the production of events with top quarks, low missing transverse momentum, and many additional quarks or gluons. The results of a search for new physics in events with two top quarks and additional jets are reported. The search is performed using events with at least seven jets and exactly one electron or muon. No requirement on missing transverse momentum is imposed. The study is based on a sample of proton-proton collisions at $\sqrt{s} = 13$ TeV corresponding to 137 fb^{-1} of integrated luminosity collected with the CMS detector at the LHC in 2016–2018. The data are used to determine best fit values and upper limits on the cross section for pair production of top squarks in scenarios of RPV and stealth supersymmetry. Top squark masses up to 670 (870) GeV are excluded at 95% confidence level for the RPV (stealth) scenario, and the maximum observed local signal significance is 2.8 standard deviations for the RPV scenario with top squark mass of 400 GeV.

"Published in Physical Review D as doi:10.1103/PhysRevD.104.032006."

1 Introduction

Supersymmetry [1, 2] (SUSY) is an extension of the standard model (SM) that may provide a solution to the gauge hierarchy problem [3]. In the SUSY framework, quadratically divergent radiative corrections to the Higgs boson mass parameter, dominated by loops involving the top quark, are canceled by loops with bosonic top quark superpartners (top squark, \tilde{t}). To avoid fine tuning, the lightest \tilde{t} and the superpartners of the Higgs bosons (higgsinos) must have masses near the weak scale [3–8], and could therefore have nonnegligible production cross sections at the CERN Large Hadron Collider (LHC).

Most searches for the \tilde{t} look for an excess of events with large missing transverse momentum p_T^{miss} originating from the undetected lightest SUSY particle (LSP) produced in \tilde{t} decays. It is typical in these searches to assume that the LSP is the lightest neutralino $\tilde{\chi}_1^0$, which is stable if R -parity [9] is conserved. However, it has been shown [10–12] that this search strategy is not sensitive to well-motivated SUSY models that predict signatures with low p_T^{miss} in models with gauge mediated SUSY breaking [13], compressed mass spectra [14, 15], hidden valleys [16], or other mechanisms. As searches performed at the LHC using events with high p_T^{miss} set ever more stringent lower bounds on the \tilde{t} mass [17–22], searches for low- p_T^{miss} alternatives become increasingly important.

Models of R -parity violating (RPV) SUSY produce low- p_T^{miss} signatures by providing a mechanism for the LSP, in this case $\tilde{\chi}_1^0$, to decay. Among other couplings, RPV SUSY includes a trilinear Yukawa coupling between quarks and squarks that allows the $\tilde{\chi}_1^0$ to decay into three quarks via an off-shell squark [9]. These couplings are typically referred to as λ''_{ijk} where i, j , and k specify the generations of the participating (s)quarks. The benchmark RPV model used in this analysis is illustrated in Fig. 1. The \tilde{t} decays in the typical way into a top quark and a $\tilde{\chi}_1^0$, and the $\tilde{\chi}_1^0$ undergoes an RPV decay via nonzero λ''_{112} into three light-flavor quarks, $\tilde{\chi}_1^0 \rightarrow uds$. However, since this analysis does not distinguish between jets originating from quarks of the first and second generation, our results are more broadly applicable to any RPV model with coupling λ''_{abc} with $a, b, c \in \{1, 2\}$.

Stealth SUSY models [12, 23, 24] introduce a new hidden “stealth” sector of light particles with small or absent couplings to the SUSY breaking sector and finite couplings to the visible sector. Because of the weak connection to the SUSY breaking sector, SUSY is approximately conserved in the stealth sector, resulting in stealth particles that are nearly mass-degenerate with their superpartners. Production and decay of stealth particles via interactions with visible particles can be achieved through a variety of “portals” including mediation by the Higgs boson or new particles at a higher mass scale. The benchmark stealth SUSY model used in the interpretation of the results of this search (stealth SY \bar{Y}) [24] assumes a minimal stealth sector containing only one scalar particle S with even R -parity and its superpartner \tilde{S} , both of which are singlets under all SM interactions, and a portal mediated by loop interactions involving a new vector-like messenger field (Y), the gluon (g), $\tilde{\chi}_1^0$, S , and \tilde{S} . Decays of the \tilde{t} in the stealth SY \bar{Y} model are illustrated in Fig. 1. Each \tilde{t} decays to a gluon, top quark, and \tilde{S} , with subsequent decays of \tilde{S} to S and a gravitino \tilde{G} and S to jets via $S \rightarrow gg$. Because of the small mass splitting between the S and \tilde{S} , as well as the small \tilde{G} mass, the undetected \tilde{G} carries away very little momentum. Thus, the stealth SY \bar{Y} model shares the general feature of all stealth SUSY models in that it naturally produces a low- p_T^{miss} signature without R -parity violation or a special tuning of sparticle masses.

The RPV and stealth SY \bar{Y} models are characterized by the masses of the particles and branching fractions in the decay chain. In the benchmark RPV model, we take the $\tilde{\chi}_1^0$ mass to be 100 GeV.

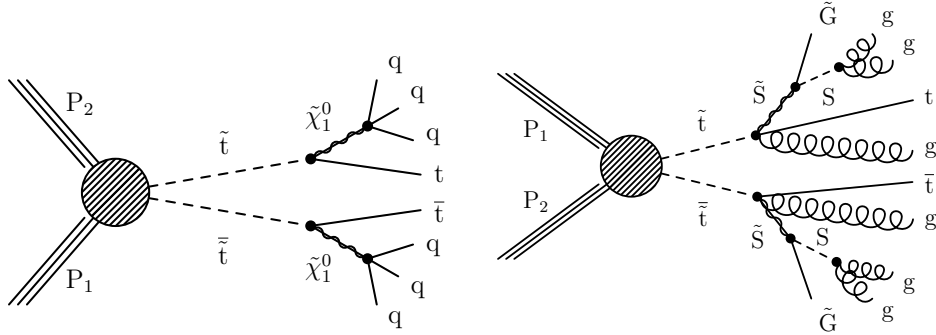


Figure 1: Diagrams of top squark pair production with decays to top quarks and additional light-flavor quarks for the RPV SUSY model (left) and with decays to top quarks and gluons for the stealth SY \tilde{Y} model (right).

For the benchmark stealth SY \tilde{Y} model, the critical small \tilde{S} - \tilde{S} mass splitting is held constant at 10 GeV, and we assume a \tilde{S} mass of 100 GeV and a \tilde{G} mass of 1 GeV. For both models, a range of \tilde{t} masses ($m_{\tilde{t}}$) are considered from 300 to 1400 GeV, and all decays described above are assumed to be prompt with unity branching fractions.

In this paper, we describe a search for $\tilde{t}\tilde{t}^*$ pair production followed by the decay of each \tilde{t} into a top quark and three light-flavor jets via the benchmark RPV and stealth SY \tilde{Y} models described above. This is the first search of its kind at the LHC. Previous searches for RPV \tilde{t} decays focused on final states with dijet resonances [25, 26], lepton-jet resonances [27, 28], intermediate leptonic chargino decays [29], or final states with many b quarks [30]. Previous searches for stealth SUSY targeted superpartners of light-flavor quarks with decays into gauge bosons and jets [31, 32]. Measurements of the $t\bar{t}$ differential production cross section have been reinterpreted in the context of RPV and stealth SUSY [24, 33] and were found to yield weak constraints for the models considered in this paper.

Before describing each step in more detail in subsequent sections, we provide an overview of the analysis strategy here. The main distinguishing feature of the signals in this analysis, in addition to the presence of two top quarks, is high jet multiplicity (N_{jets}). The SM backgrounds arise through processes including top quark pair production ($t\bar{t}$), multijet production from quantum chromodynamics (QCD), production of $t\bar{t}$ in association with SM weak gauge bosons or additional top quarks ($t\bar{t}+X$), production of weak gauge bosons, and single top quark production (other). These SM processes all include additional jets from initial- and final-state radiation (ISR and FSR). The QCD background is primarily suppressed by requiring the presence of exactly one charged lepton (e or μ) arising from the leptonic decay of a top quark. Backgrounds that do not produce any top quarks are suppressed by requiring the presence of at least one jet identified as arising from the fragmentation of a bottom quark (b-tagged jet), and additionally that the invariant mass of the lepton and a b-tagged jet be consistent with the presence of a top quark.

The signal is distinguished from the dominant and irreducible $t\bar{t}$ background by means of a neural network (NN) trained to recognize differences in the spatial distribution of jets and decay kinematic distributions between signal and $t\bar{t}$ background events. Events are divided into 24 categories based on their NN score (S_{NN}) and N_{jets} ; categories with higher (lower) S_{NN} and N_{jets} tend to be signal enriched (depleted). We perform a simultaneous fit to the number of events in data in S_{NN} and N_{jets} categories to estimate the total numbers of $t\bar{t}$ and potential signal events present in the data, as well as the distribution of $t\bar{t}$ events in S_{NN} and N_{jets} categories.

The NN output is designed to have no dependence on N_{jets} , so that the N_{jets} distribution of $t\bar{t}$ events can be constrained in the fit to be the same for all S_{NN} categories. This requirement for $t\bar{t}$ N_{jets} shape invariance is important for the analysis and will be discussed throughout the paper.

This paper is organized as follows. We introduce the CMS detector and methods for event reconstruction and selection in Section 2. Samples of simulated events are described in Section 3. The estimation and modeling of SM backgrounds are explained in Section 4, and the description of the treatment of systematic uncertainties is in Section 5. Finally, the results and their interpretation are in Section 6, followed by the summary in Section 7.

2 Experimental techniques

The search is performed using a data sample of proton-proton (pp) collisions at $\sqrt{s} = 13$ TeV, corresponding to an integrated luminosity of 137 fb^{-1} , collected in 2016–2018 with the CMS detector at the LHC. Data and simulation samples from four periods (2016, 2017, 2018A, 2018B) are treated separately in order to address variations in detector and LHC conditions. Data from 2018 are divided into two samples (2018A and 2018B), with 2018B corresponding to the period when a detector malfunction prevented readout from 3% of the hadron calorimeter. In this section, we define reconstructed physics objects and describe the selection criteria for events in the signal region (SR) and the control region (CR) of the analysis.

The central feature of the CMS apparatus is a superconducting solenoid of 6 m internal diameter, providing a magnetic field of 3.8 T. Within the solenoid volume are a silicon pixel and strip tracker, a lead tungstate crystal electromagnetic calorimeter, and a brass and scintillator hadron calorimeter, each composed of a barrel and two endcap sections. Forward calorimeters extend the pseudorapidity coverage provided by the barrel and endcap detectors. Muons are detected in gas-ionization chambers embedded in the steel flux-return yoke outside the solenoid. A more detailed description of the CMS detector, together with a definition of the coordinate system used and the relevant kinematic variables, can be found in Ref. [34].

The CMS trigger system is described in Ref. [35]. Events are selected using triggers that require the presence of at least one electron or one muon. The minimum transverse momentum p_{T} threshold is 27 (35) GeV for electrons and 24 (24) GeV for muons in 2016 (2017–2018). The triggers at these thresholds require the lepton to be isolated from tracks and calorimeter deposits in the detector. Events may also be selected from single-lepton triggers with higher p_{T} thresholds, 115 GeV for electrons and 50 GeV for muons, with no isolation requirements. The combined trigger efficiency varies from 80% for leptons with p_{T} close to the lower thresholds to greater than 95% for leptons with $p_{\text{T}} > 120$ GeV.

Events are reconstructed using the particle-flow (PF) algorithm [36], which reconstructs particles in an event using an optimized combination of information from the various elements of the CMS detector and identifies each as a photon, electron, muon, charged hadron, or neutral hadron. These particles are further clustered into jets as described below.

The reconstructed vertex with the largest value of summed physics-object p_{T}^2 is taken to be the primary pp interaction vertex, where the physics objects are the jets, clustered using the anti- k_{T} algorithm [37, 38] with the charged-particle tracks assigned to the vertex as inputs, and the associated missing transverse momentum, taken as the negative vector sum of the p_{T} of those jets [39]. Charged-particle tracks associated with vertices from other pp interactions (pileup) are removed from further consideration. The primary vertex is required to lie within 24 cm of the interaction point along the beam axis, and within 2 cm in the plane transverse to the beam

axis.

Electrons and muons must satisfy $p_T > 30 \text{ GeV}$ and $|\eta| < 2.4$. For the analysis of the 2017 and 2018 data, the electron p_T threshold is increased to 37 GeV to account for the higher trigger threshold. The lepton identification requirements are the “tight” criteria for electrons [40] and the “medium” criteria for muons [41]. Leptons must be isolated within a cone of radius $R = \sqrt{(\Delta\phi)^2 + (\Delta\eta)^2}$ that scales as $1/p_T$ between a maximum of 0.2 for leptons with $p_T < 50 \text{ GeV}$ and a minimum of 0.05 for lepton $p_T > 200 \text{ GeV}$ [42].

Jets are clustered from the reconstructed PF particles using the anti- k_T algorithm with a distance parameter of 0.4. Criteria are applied to remove events with jets arising from instrumental effects or reconstruction failures [43, 44]. The reconstructed jet energies are corrected for the nonlinear response of the detector [45, 46] and for contributions from neutral hadrons from pileup [47]. Jets are required to have $p_T > 30 \text{ GeV}$ and $|\eta| < 2.4$. Jets overlapping with a selected lepton within a cone of radius $R = 0.4$ are removed. A neural network-based algorithm [48] is used to identify b quark jets; for jets with p_T around 30 GeV , the algorithm has an efficiency of 65% and a misidentification rate for light-flavor jets (including gluon jets) of 1%.

In addition to the trigger and vertex criteria above, events in the SR must contain exactly one isolated electron or muon and at least seven jets, at least one of which should be b tagged. Samples with seven and eight jets include a small number of expected signal events, but are included in the SR to constrain the background. To further reject the QCD background, we require the scalar sum of jet p_T (H_T) to exceed 300 GeV . To suppress non- $t\bar{t}$ backgrounds, we require the invariant mass of the system formed by the b-tagged jet and the lepton to be between 50 and 250 GeV . If there is more than one b-tagged jet in the event, the invariant mass of each b-tagged jet and the lepton is considered, and at least one combination is required to meet the above criterion. No requirement is made on the event p_T^{miss} .

In addition to the SR, a signal-depleted control region (CR) dominated by QCD background is defined with the dual purpose of determining the QCD contribution to the SR and verifying the important assumption of $t\bar{t} N_{\text{jets}}$ shape invariance with S_{NN} . Despite being dominated by QCD background, the CR is useful for confirming $t\bar{t} N_{\text{jets}}$ shape invariance because many of the jets used as inputs to the NN arise from QCD radiation, which is common to the $t\bar{t}$ and QCD backgrounds; this claim is verified in Section 5. The CR is defined similarly to the SR with the differences being that the lepton is required to be a muon; the muon is required to fail the SR isolation requirement; there is no requirement for a b-tagged jet, nor on the invariant mass of the lepton and b-tagged jet; the only trigger used is the high-threshold muon trigger without an isolation requirement; and the muon p_T threshold is 55 GeV .

3 Simulated event samples

Simulated event samples are used in the estimation of the expected number of SM background and signal events passing the SR selection. Top quark pair and single top quark events produced in the t channel are generated with the next-to-leading-order (NLO) POWHEG v2.0 [49–53] generator, while single top quark events in the tW channel are generated with POWHEG v1.0 [52]. Single top quark production in the s channel, as well as rare SM processes such as $t\bar{t}Z$ and $t\bar{t}W$ are generated at NLO accuracy with the MADGRAPH5_aMC@NLO v2.2.2 program. The MADGRAPH5_aMC@NLO v2.2.2 generator [54, 55] is used in the leading-order (LO) mode to simulate QCD and W +jets events.

For the signal, top squark pair production events are generated using MADGRAPH5_aMC@NLO

in LO mode, including up to two additional partons in the matrix element calculation. The top squarks are decayed using PYTHIA v8.212 (2016) or 8.226 (2017–2018) [56] according to the signal models described in Section 1. The signal production cross section ($\sigma_{\bar{t}t}$) is calculated as a function of $m_{\bar{t}}$ using approximate next-to-NLO (NNLO) plus next-to-next-to-leading-logarithm (NNLL) calculations [57, 58].

The generation of these processes is based on either LO or NLO parton distribution functions (PDFs) using NNPDF3.0 [59] for the simulated samples corresponding to 2016 detector conditions, and using the NNLO PDF sets from NNPDF3.1 [60] for the 2017 and 2018 simulated samples. Parton showering and hadronization are simulated with PYTHIA using underlying event tune CUETP8M1 [61] for 2016 samples, except for $\bar{t}t$ production which used tune CUETP8M2T4 [62], or PYTHIA with tune CP5 (CP2) [63] for all 2017 and 2018 background (signal) samples. To model the effects of pileup, simulated events are generated with a nominal distribution of pp interactions per bunch crossing and then reweighted to match the corresponding distribution in data. The CMS detector response is simulated using a GEANT4-based model [64], and event reconstruction is performed in the same manner as for collision data. The most precise cross section calculations available are used to normalize the SM simulated samples, corresponding to NLO or NNLO accuracy in most cases [54, 65–71].

The simulation is corrected to eliminate small discrepancies between data and simulation in the trigger efficiency, lepton selection efficiency, and b tagging efficiency. Analysis-specific corrections for the H_T distribution in $\bar{t}t$ simulation, parameterized as functions of N_{jets} and H_T , are obtained in a signal-depleted sample identical to the SR, except for the requirement $5 \leq N_{\text{jets}} \leq 7$. Events with $N_{\text{jets}} = 7$ are common to the SR, but as mentioned above, this sample has low signal contamination. The correction is parameterized with an exponential function in H_T with parameters depending linearly on N_{jets} in order to extend the correction into the $N_{\text{jets}} > 7$ SR. The H_T correction is small at low H_T and 20–40% at $H_T = 1500$ GeV, depending on N_{jets} .

4 Background estimation

Simulated background events passing the SR selection requirements predominantly originate from $\bar{t}t$ production, with contributions of less than 10% from QCD, and a few percent from the remaining minor backgrounds including $\bar{t}t$ production in association with a vector boson, single top quark production, and $W + \text{jets}$.

As introduced in Section 1, the crux of the analysis is to estimate the dominant $\bar{t}t$ background in four bins of S_{NN} and six N_{jets} bins using a simultaneous binned maximum-likelihood fit constraining the $\bar{t}t$ N_{jets} shape to be the same in all S_{NN} categories. Event yields, as well as the N_{jets} and S_{NN} distributions, are fixed at values determined from a signal-depleted data control sample for the QCD background and from simulation for the minor backgrounds, as described later in this section. The yield and N_{jets} shape of the $\bar{t}t$ background, along with the signal strength, are determined in the fit; signal strength is defined as the ratio of the fit signal event yield to the one predicted by SUSY.

The NN is trained to discriminate between signal and $\bar{t}t$ background by exploiting differences in the event shape and distributions of the kinematic variables. The gradient reversal technique [72] is used to minimize dependence of the NN output on N_{jets} , as required by the primary assumption that the $\bar{t}t$ N_{jets} shape is the same in all S_{NN} categories. All NN input variables are computed in an approximate center-of-mass frame defined by all jets in the event with $p_T > 30$ GeV and $|\eta| < 5$. The NN input variables include the four-vector components

for the seven jets in the event with the highest momentum in the center-of-mass frame, the four-vector components of the lepton in the event, the second through fifth Fox–Wolfram moments [73] normalized by the first moment, and the three eigenvalues of the sphericity tensor [74] normalized by the sum of the eigenvalues. The Fox–Wolfram moments and sphericity tensor eigenvalues, which are computed from the same seven highest momentum jets, quantify the distribution of jet energy in the event, which tends to be more spherical for signal $\bar{t}t$ pair production than for the $t\bar{t}$ background.

For the NN training, simulated $t\bar{t}$ events are used for the background sample, and a mixture of RPV and stealth $SY\bar{Y}$ simulated events with $m_{\bar{\tau}}$ from 350–850 GeV is used as the signal sample. In this way, the NN can identify common features among all signal samples ensuring a search with broad sensitivity. Reflecting differences in simulation between the data taking periods, as described in Section 3, a single training is used for 2017, 2018A, and 2018B, with a separate training used for 2016. The S_{NN} distributions for the simulated background, several signal models, and the 2016 and 2017+2018 data are shown in Fig. 2.

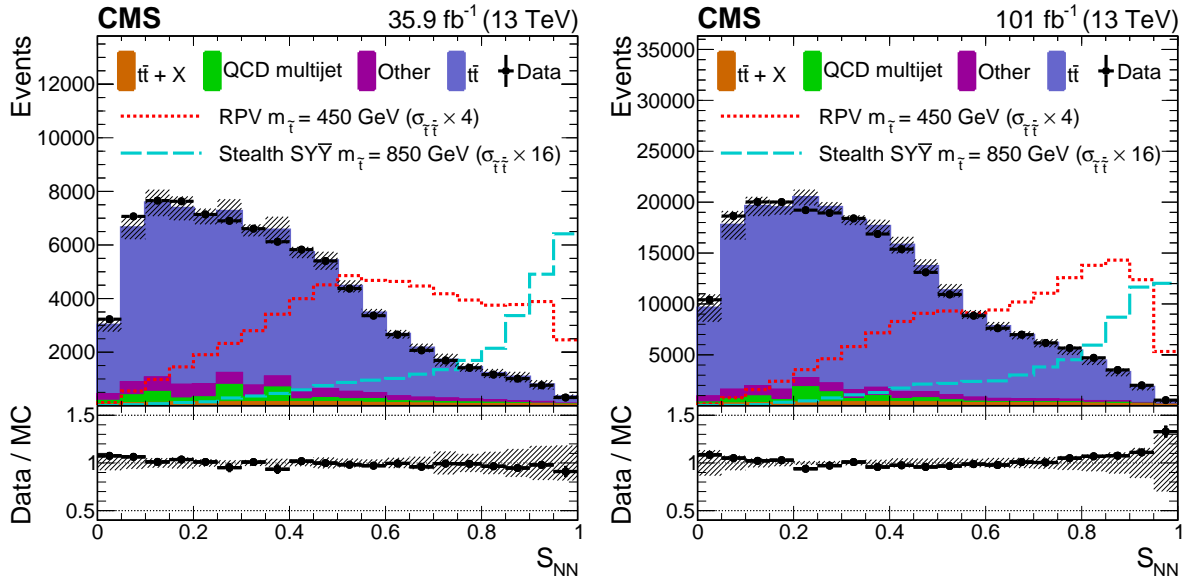


Figure 2: The S_{NN} distributions for the 2016 training (left) and 2017+2018 training (right) show the corresponding data in the SR (black points); simulated background normalized to the number of data events (filled histograms); RPV signal model with $m_{\bar{\tau}}$ of 450 GeV (red short dashed); and stealth $SY\bar{Y}$ signal model with $m_{\bar{\tau}}$ of 850 GeV (cyan long dashed). All events shown pass the SR event selection. The band on the total background histogram denotes the dominant systematic uncertainties related to the modeling of H_T , jet mass, and jet p_T in the $t\bar{t}$ simulation, as well as the statistical uncertainty for the non- $t\bar{t}$ components. The lower panel shows the ratio of the number of data events to the number of normalized simulated events with the band representing the difference between the nominal ratio and the ratio obtained when varying the total background by its uncertainty.

For each of the six N_{jets} bins, events are divided into four S_{NN} bins: $S_{NN,1}$ (lowest S_{NN}), \dots , $S_{NN,4}$ (highest S_{NN}). The S_{NN} bin boundaries are chosen separately for each N_{jets} bin such that the expected significance for the 550 GeV RPV signal model, which has expected significance close to 5 standard deviations (σ), is maximized, under the constraint that the fraction of simulated $t\bar{t}$ events in each S_{NN} bin is the same for all N_{jets} bins. For example, the fraction of all events in each N_{jets} bin falling into the $S_{NN,1}$ bin is constrained to be approximately 56%, while the fraction of events falling into the $S_{NN,4}$ bin is constrained to be approximately 2.4%. This

constraint removes the small dependence of S_{NN} on N_{jets} that remains after NN training with gradient reversal.

In the maximum-likelihood fit, the $t\bar{t}$ N_{jets} distribution is parameterized with a function inspired by QCD jet scaling patterns [75] in which the ratio $R(i) = M_{i+1}/M_i$, where M_i is the number of events with $N_{\text{jets}} = i$, can be described by a falling ‘‘Poisson’’ component at low N_{jets} and a constant ‘‘staircase’’ component at high N_{jets} . This ratio is well modeled by the function

$$f(i) = a_2 + \left[\frac{(a_1 - a_2)^{i-7}}{(a_0 - a_2)^{i-9}} \right]^{1/2}.$$

Notice that $a_0 = f(7)$, $a_1 = f(9)$, and a_2 is the asymptotic value for large i . This particular parameterization was chosen to avoid large correlations between the fit parameters. The N_{jets} distribution for each S_{NN} bin j (see Fig. 4) is modeled using a recursive expression given by $M_i^j = Y_7^j \prod_{k=7}^{i-1} f(k)$ where Y_7^j are normalization parameters that are floating in the fit. The last N_{jets} bin considered is an inclusive $N_{\text{jets}} \geq 12$ bin, such that $i \in [7, 12]$. In the maximum-likelihood fit, the free parameters consist of the three shape parameters a_0 , a_1 , and a_2 ; the four normalization parameters Y_7^j ; the signal strength; and all nuisance parameters related to systematic uncertainties described in Section 5.

The QCD background yield parameters are fixed in the fit at the values determined from the CR. More specifically, the QCD background prediction for each $N_{\text{jets}}-S_{\text{NN}}$ bin in the SR is given by the yield for the same bin in the CR in data, after subtraction of the non-QCD backgrounds as predicted from simulation, multiplied by the ratio of SR to CR yields in simulation (R_{QCD}). This procedure is verified with a closure test in the simulation. The yield parameters from the minor backgrounds are also kept fixed in the fit at the values predicted by simulation. While the yield parameters are fixed in the fit, the ultimate contributions from QCD and minor backgrounds vary according to the constrained nuisance parameters related to systematic uncertainties in those fit components.

5 Systematic uncertainties and fit validation

As described in Section 4, an unbiased estimate of the dominant $t\bar{t}$ background is obtained from the fit to data as long as the $t\bar{t}$ N_{jets} shape is the same for all four S_{NN} bins. By construction, N_{jets} shape invariance is achieved in the simulation with an N_{jets} -specific S_{NN} binning as described in the previous section. Thus, systematic uncertainties on the $t\bar{t}$ background are important to the degree that they violate the assumption that the S_{NN} binning determined in simulation also applies to the data. We quantify how each source of uncertainty causes deviations from the assumed N_{jets} shape invariance by comparing the nominal N_{jets} shape to the N_{jets} shapes in all S_{NN} bins after performing the relevant systematic variation to the $t\bar{t}$ simulation. Each systematic variation is associated with a constrained nuisance parameter in the fit. The deviation in shape for each N_{jets} distribution, derived from the ratio of the post-variation shape divided by the nominal shape, changes linearly with the associated nuisance parameter for the systematic variation, while preserving the normalization of the distribution.

Sources of $t\bar{t}$ shape uncertainty include uncertainty in aspects of event generation including PDFs, choice of renormalization and factorization scales (μ_{R} , μ_{F} scales), and parton shower modeling, which is itself composed of aspects related to modeling of ISR, FSR, color reconnection in the parton shower, matrix element-parton shower matching scale (ME-PS), underlying event (UE tune), and pileup modeling. The uncertainty due to the choice in (μ_{R} , μ_{F}) scales is

determined by independently varying both by factors of 2.0 and 0.5 excluding the variations (2.0, 0.5) and (0.5, 2.0) [55, 76, 77]. The ISR and FSR uncertainties originate from variations of the renormalization scale for the parton shower by factors 0.5 and 2.0, effectively varying the value of α_S . The color reconnection uncertainty is calculated by allowing resonant decays to occur before the merging of multi-parton systems. The ME-PS uncertainty is obtained by varying the POWHEG parameter that governs ME-PS matching about its nominal value according to $h_{\text{damp}} = 1.379^{+0.926}_{-0.505}$ times the top quark mass [63]. The UE tune uncertainty comes from variation of the PYTHIA parameters that control the modeling of the underlying event as described in Ref. [63]. The total inelastic pp cross section is changed by 5% to estimate the uncertainty related to pileup [78].

Sources of $t\bar{t}$ shape uncertainty related mostly to aspects of detector simulation include determination of jet energy scale (JES) and resolution (JER), modeling of the b tagging efficiency, modeling of the efficiency for lepton triggers, identification, and isolation (lepton efficiencies); residual mismodeling of H_T , jet p_T , and jet mass; and use of the CR for measuring deviations from the assumption of N_{jets} shape invariance.

The uncertainty in the modeling of H_T in the $t\bar{t}$ simulation is composed of four separate components. The first H_T uncertainty (primary) is taken as the full difference in the $t\bar{t}$ background shape with and without the H_T correction. The second H_T uncertainty (validation) is taken as the difference between the simulation with nominal H_T correction (described in Section 3) and the observed H_T distribution in the signal-depleted SR sample with $N_{\text{jets}} = 8$. The third and fourth H_T uncertainties address the choices of parameterization of the H_T correction as functions of H_T and N_{jets} . For these, we take the uncertainty as the difference between the nominal correction and two alternate corrections that use the $H_T = 2000$ GeV correction for all events with $H_T > 2000$ GeV (H_T -parameterization) and the $N_{\text{jets}} = 7$ correction for all values of N_{jets} (N_{jets} -parameterization).

Comparisons of data and simulation in the CR show that the simulation predicts distributions with higher values of jet p_T and mass than observed. The observed discrepancy at jet p_T (mass) of 400 (50) GeV depends on jet p_T rank and is small for the highest p_T jet in each event growing to approximately 50% for the jet with sixth-highest p_T in each event. Similar trends are observed in the signal-depleted, $t\bar{t}$ -dominated SR with $N_{\text{jets}} = 7$. In the CR, the discrepancy in the falling tail of each distribution is minimized when the p_T (mass) of each jet is scaled by the value 0.95, 0.95, 0.95, 0.95 (0.95, 1.01, 0.98, 0.98) for 2016, 2017, 2018A, and 2018B, respectively. Thus, the related $t\bar{t}$ shape uncertainty is taken to be the resulting difference between scaled and nominal simulated $t\bar{t}$ distributions. The dependence on jet p_T rank indicates that the discrepancy arises predominantly in the event generation; however, we choose to estimate the associated systematic uncertainty separately for each data taking period to include potential effects of detector response simulation. The H_T correction is omitted from the determination of these jet p_T and mass uncertainties to avoid double counting of H_T mismodeling effects. In addition, because the estimation of jet p_T and mass uncertainties relies on variable scaling (rather than event reweighting), the uncertainties include effects of changes in the S_{NN} for each event, which is not included in the H_T uncertainty.

As mentioned above, the use of N_{jets} -dependent S_{NN} binning ensures that the N_{jets} shape is the same in all four S_{NN} bins in simulation, and the use of the same binning in the data assumes that the N_{jets} - S_{NN} dependence is well modeled in the simulation. This assumption is confirmed and a related systematic uncertainty is determined by comparing the N_{jets} shapes (in five uniform S_{NN} bins) for data and simulation in the CR. For each of the six N_{jets} bins, we compute the ratio $R_M = (1/\mu_i) (M_{\text{all}}/M_i)$ as a function of S_{NN} , where M_{all} is the total number

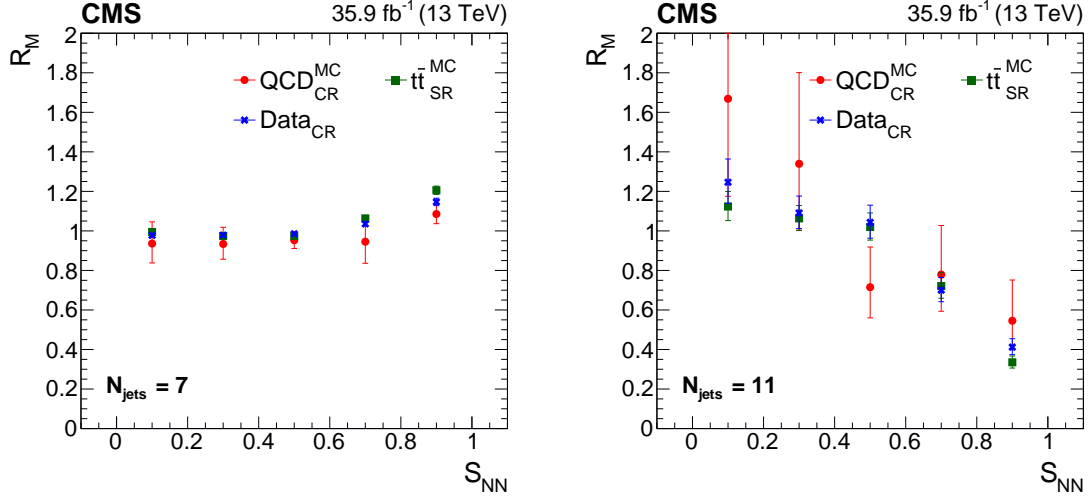


Figure 3: Distribution in S_{NN} of the ratio R_M , as defined in the text, for $N_{\text{jets}} = 7$ (left) and 11 (right), for the QCD CR simulation (red circles), the $\text{t}\bar{\text{t}}$ SR simulation (green squares), and data in the CR (blue crosses) for the 2016 data period. The error bars indicate the statistical uncertainty in the value of R_M .

of events in all N_{jets} bins, M_i is the total number of events in the $N_{\text{jets}} = i$ bin, and μ_i is the uncertainty-weighted average of M_{all}/M_i in the $N_{\text{jets}} = i$ bin used to facilitate comparison of the R_M shapes between samples and N_{jets} bins with different normalizations. Figure 3 shows a comparison of R_M (from $N_{\text{jets}} = 7$ and 11 in the 2016 analysis) for simulation of the QCD background in the CR ($\text{QCD}_{\text{CR}}^{\text{MC}}$), simulation of $\text{t}\bar{\text{t}}$ in the SR ($\text{t}\bar{\text{t}}_{\text{SR}}^{\text{MC}}$), and the data in the QCD background-dominated CR (Data_{CR}). Agreement between $\text{QCD}_{\text{CR}}^{\text{MC}}$ and $\text{t}\bar{\text{t}}_{\text{SR}}^{\text{MC}}$ demonstrates that QCD background-dominated data in the CR are a good proxy for $\text{t}\bar{\text{t}}$ -dominated data in the SR, and agreement between $\text{QCD}_{\text{CR}}^{\text{MC}}$ and Data_{CR} verifies that the dependence of the N_{jets} shape on S_{NN} is well modeled in the simulation. Similar agreement is found for the R_M distributions for the other N_{jets} bins and data periods. The uncertainty related to the combination of both effects is taken as the difference between $\text{t}\bar{\text{t}}_{\text{SR}}^{\text{MC}}$ and Data_{CR} .

For the QCD background, the shape is obtained from data in the CR, and the normalization is set with R_{QCD} . Because the systematic uncertainties in the simulation largely cancel in the R_{QCD} ratio, the uncertainty in R_{QCD} is dominated by the statistical uncertainty of simulated samples and ranges from 15–25% depending on data collection period.

Sources of systematic uncertainty in the predictions for signals and the minor backgrounds include PDFs, JES, JER, b tagging efficiency, lepton efficiency, trigger efficiency, (μ_R, μ_F) scales, cross sections for the minor backgrounds, and a 2.3–2.5% uncertainty in the integrated luminosity [79–81]. Since the signal and minor backgrounds are estimated directly from simulation, related uncertainties are included as the full effect of the systematic variation on the yields in each N_{jets} and S_{NN} bin, thereby taking into account normalization effects as well as shape changes.

Uncertainties derived from comparisons of data and simulation separately in each data taking period (related to pileup, JES, JER, b tagging efficiency, lepton efficiencies, H_T corrections, N_{jets} shape invariance, and integrated luminosity) are treated as uncorrelated among all data samples. Uncertainties related to parton shower modeling are treated as fully correlated for 2017, 2018A, and 2018B, while the corresponding uncertainties for 2016 are uncorrelated with those

from the other data taking periods; uncertainties related to (μ_R, μ_F) scales and cross sections for the minor backgrounds are treated as correlated between all four periods.

Table 1 shows the impact of the systematic uncertainties on the expected event yields for the $t\bar{t}$ background, minor backgrounds, and the RPV signal model with $m_{\tilde{t}} = 550$ GeV. For sources of uncertainty for which the size of the impact depends on N_{jets} and S_{NN} , a representative range of values is listed along with the maximum value from all bins.

Table 1: Summary of the impact of systematic uncertainties in the expected event yields for the $t\bar{t}$ background, minor backgrounds (both $t\bar{t}+X$ and other), and the RPV signal model with $m_{\tilde{t}} = 550$ GeV. Abbreviated names for each source of uncertainty are explained in the text. For sources of uncertainty for which the size of the impact depends on N_{jets} and S_{NN} , a representative range of values showing the 16th and 84th percentile of all the corrections is listed with the maximum value from all bins shown in parentheses. All values are in units of percent.

Source of uncertainty	$t\bar{t}$ background	Minor background	RPV signal
PDFs	0–1 (2)	0–1 (8)	0–2 (7)
(μ_R, μ_F) scales	0–2 (5)	1–8 (18)	0–3 (4)
ISR	0–4 (15)	—	—
FSR	0–8 (27)	—	—
Color reconnection	0–10 (44)	—	—
ME-PS	0–14 (82)	—	—
UE tune	0–7 (100)	—	—
Pileup	0–2 (7)	0–7 (28)	0–2 (4)
JES	0–4 (18)	5–21 (100)	1–11 (31)
JER	0–2 (10)	1–15 (100)	0–6 (14)
b tagging	0–1 (3)	0–2 (12)	0–2 (2)
Lepton efficiencies	0–1 (1)	3–5 (5)	3–4 (4)
H_T primary	0–5 (17)	—	—
H_T validation	0–1 (4)	0–6 (10)	—
H_T H_T -parameterization	0–2 (9)	—	—
H_T N_{jets} -parameterization	0–7 (27)	—	—
Jet p_T	0–4 (15)	—	—
Jet mass	0–4 (15)	—	—
N_{jets} shape invariance	0–12 (37)	—	—
Integrated luminosity	—	2.3–2.5	2.3–2.5
Theoretical cross section	—	30	—

6 Results and interpretation

The results of the fit to 2016, 2017, 2018A, and 2018B data sets with the signal strength fixed to zero (background-only fit) are shown along with the observed number of events in Fig. 4; each column (row) in the plot array corresponds to a specific S_{NN} bin (data set). The expected distributions for top squark pair production in the specific RPV ($m_{\tilde{t}} = 450$ GeV) and stealth SY \bar{Y} models ($m_{\tilde{t}} = 850$ GeV) described in Section 1 are overlaid for illustration purposes. The lower panel of each plot displays the difference between the observed number of events and the total number of expected events determined by the fit divided by the statistical uncertainty associated with the observed number of events (δ) as black points with error bars denoting δ . The

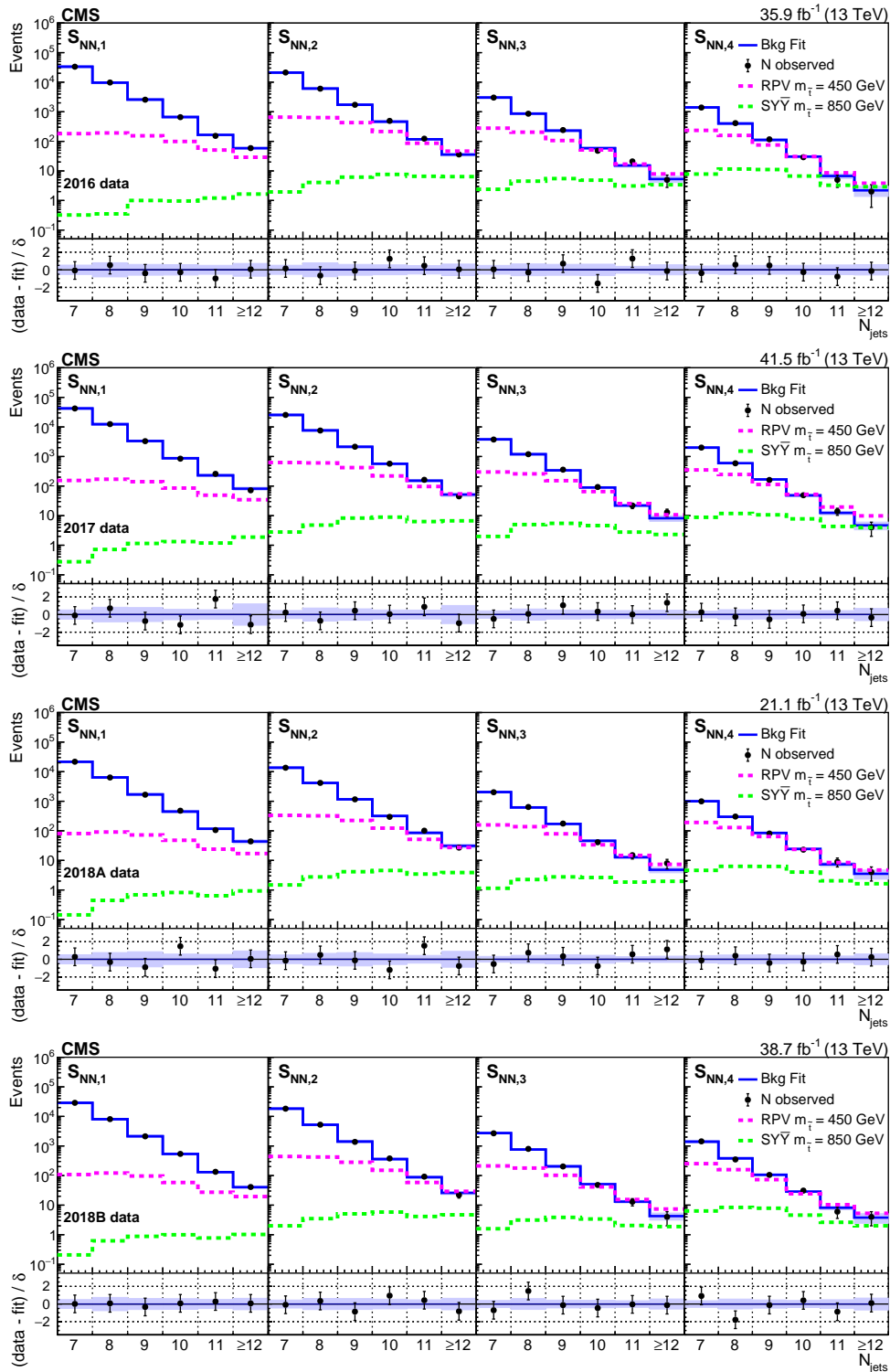


Figure 4: Fitted background prediction and observed data counts for 2016, 2017, 2018A, and 2018B (from upper to lower rows) as functions of N_{jets} in each of the four bins in S_{NN} . The signal distributions normalized to the predicted cross section for the RPV model with $m_{\tilde{\tau}} = 450$ GeV and the stealth $\text{SY}\bar{\text{Y}}$ model with $m_{\tilde{\tau}} = 850$ GeV are shown for comparison. The lower panel of each plot displays the difference between the number of observed events and the number of events determined by the fit divided by the statistical uncertainty associated with the observed number of events (δ) as black points with error bars denoting δ . The blue band shows the total systematic uncertainty in the fit from all nuisance parameters.

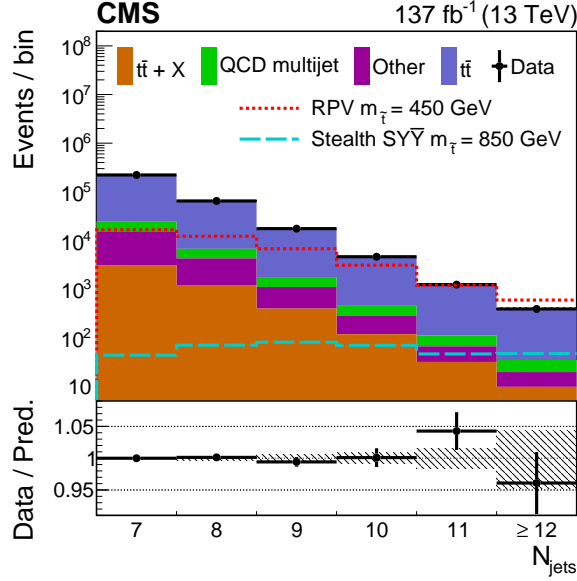


Figure 5: Background prediction from the background-only fit and observed data counts as a function of N_{jets} summed over data periods and S_{NN} bins. Overlaid are expected distributions for the RPV and stealth SY \bar{Y} models with $m_{\tilde{t}} = 450$ and 850 GeV, respectively, normalized according to the top squark pair production cross section. For visualization purposes, the hatched band in the lower panel shows the quadrature sum of all of the uncertainties on the background prediction.

blue band shows the total uncertainty in the fit determined from the full fit covariance matrix in order to account for the correlations among fit parameters. Figure 5 shows the results of the same background-only fit summed over S_{NN} bins and data periods with separate contributions from each background.

The data are also used to determine the 95% confidence level (CL) upper limits on $\sigma_{\tilde{t}\tilde{t}}$ and the signal strength p -values [82] for both the RPV and stealth SY \bar{Y} models obtained using the CL_s approach [83–85] with asymptotic formulae [86] and the profile likelihood ratio as the test statistic. Figure 6 shows the expected and observed cross section limits as a function of $m_{\tilde{t}}$ for the benchmark RPV and stealth SY \bar{Y} signal models. Comparing to the predicted cross section, these limits correspond to the exclusion of top squark masses in the range 300–670 and 300–870 GeV for the benchmark RPV and stealth SY \bar{Y} models, respectively. Figure 7 shows the local p -value [82] of the signal strength, as a function of $m_{\tilde{t}}$, obtained from fits to the data with each signal strength as a free parameter for both the RPV and stealth SY \bar{Y} models. The p -value quantifies the probability for the background to produce an upward fluctuation at least as large as that observed. Fits are performed and p -values obtained separately for each data set, as well as in a simultaneous fit to all data sets. We observe the most extreme p -value to be 0.003, which corresponds to a local significance of 2.8σ and a best fit signal strength of 0.21 ± 0.07 for the RPV model with $m_{\tilde{t}} = 400$ GeV assuming unity branching fractions for the decays described in Section 1.

The 2.8σ local significance for the RPV model with $m_{\tilde{t}} = 400$ GeV is understood to arise from a combination of two effects. First, although the level of agreement between the observed data and the background expectation shown in Fig. 4 is reasonable, the agreement improves when the signal is included in the fit, contributing approximately 1.1σ to the significance. Second, the constrained nuisance parameters (NP) are pulled less from their initial values when the signal

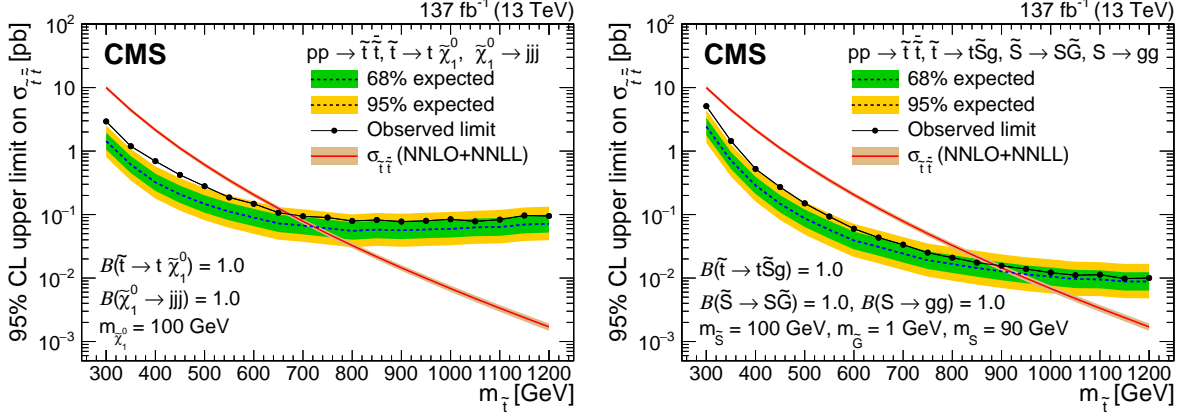


Figure 6: Expected and observed 95% CL upper limit on the top squark pair production cross section as a function of the top squark mass for the RPV (left) and stealth $SY\bar{Y}$ (right) SUSY models. Particle masses and branching fractions assumed for each model are included on each plot. The expected cross section computed at NNLO+NNLL accuracy is shown in the red curve.

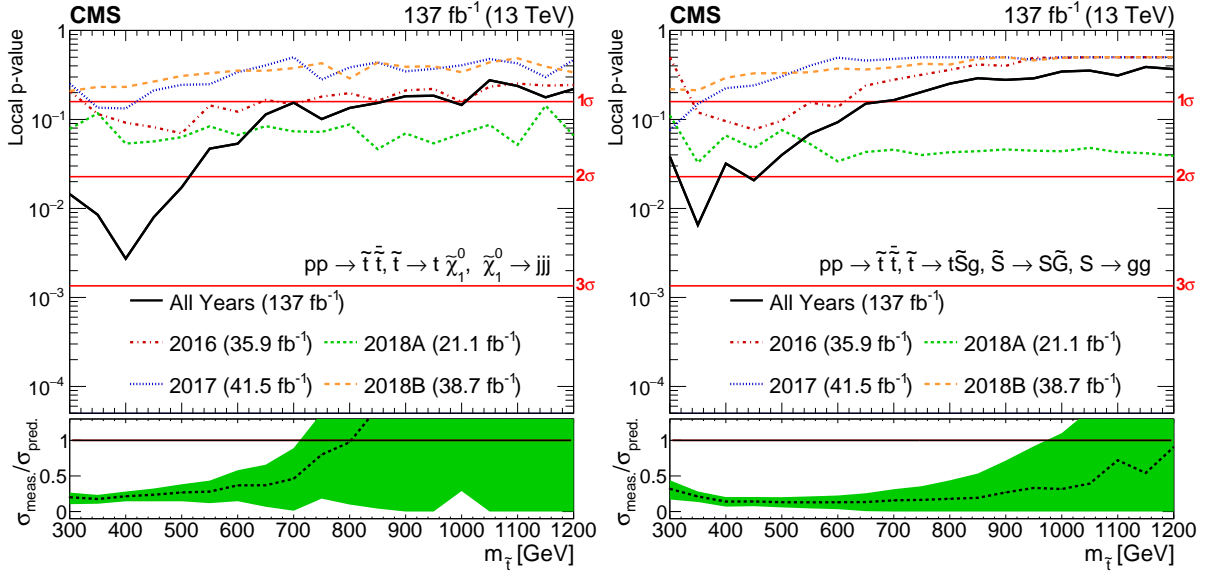


Figure 7: Local p -value as a function of top squark mass for the RPV (left) and stealth $SY\bar{Y}$ models (right). The colored lines show the p -values for separate fits of the 2016 (red dash dotted), 2017 (blue dotted), 2018A (green short dashed), and 2018B (orange long dashed) data sets; the black line shows the p -value for the simultaneous fit of data sets. The lower panels show the best fit signal strength ($\sigma_{\text{meas.}}/\sigma_{\text{pred.}}$) as a function of top squark mass with uncertainty denoted by the green band.

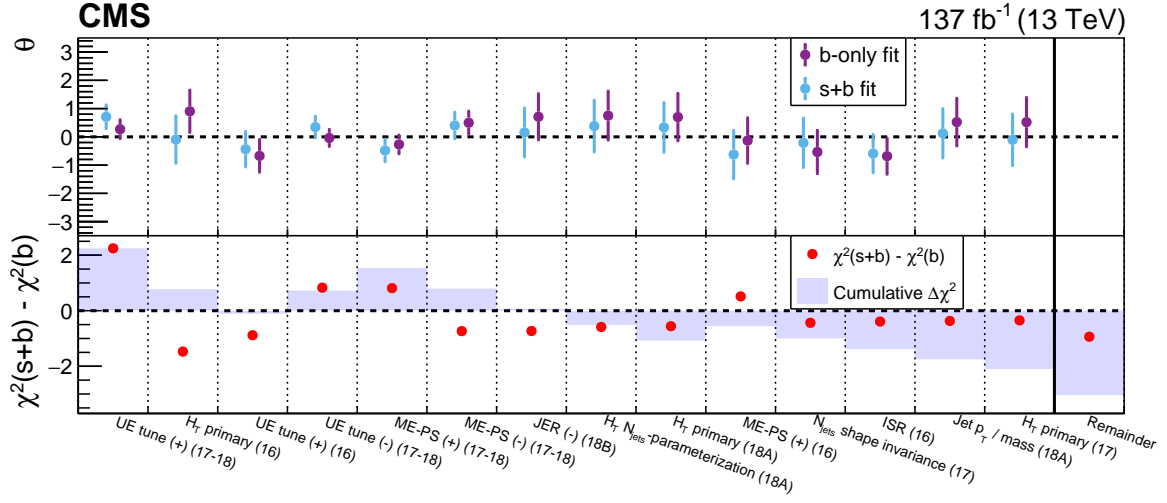


Figure 8: The upper panel shows the fit values (θ) and uncertainties (δ_θ) for a selection of nuisance parameters (NP) from both the background-only fit (purple) and signal+background fit (blue) for the RPV model with $m_{\tilde{t}} = 400$ GeV. The x-axis labels refer to the NP sources described in Section 5, the data period (16, 17, etc.), and the direction of variation (+, -). The lower panel shows the $\Delta\chi^2 \equiv \chi^2(s+b) - \chi^2(b)$ difference of $\chi^2 \equiv (\theta/\delta_\theta)^2$ from the signal+background (s+b) and background-only (b) fits as a red point for each NP and the cumulative sum of $\Delta\chi^2$ from left to right as a blue shaded histogram. The fourteen selected NP are those with $|\Delta\chi^2| > 0.3$, and the NP are ordered from left to right by decreasing $|\Delta\chi^2|$. The rightmost bin, separated by a vertical solid line, shows the sum of $\Delta\chi^2$ for all NP not displayed in the figure (red point) and the sum of $\Delta\chi^2$ for all NP (blue shaded histogram).

is included in the fit, contributing approximately 1.7σ to the significance. This second effect is illustrated in Fig. 8 which shows for each of a selection of NP: the fit value (θ) and uncertainty (δ_θ) from both the background-only fit (b) and the signal+background fit (s+b), as well as the $\Delta\chi^2 \equiv \chi^2(s+b) - \chi^2(b)$ difference of $\chi^2 \equiv (\theta/\delta_\theta)^2$ from the two fits. A θ value of one indicates that the fit value of the nuisance parameter is one standard deviation from its nominal value, and a δ_θ value less than one shows that the uncertainty is reduced in the fit relative to its initial value. All NPs have θ values below one for the background-only fit, and several NPs related to $t\bar{t}$ modeling are constrained with δ_θ in the range of 0.25–0.40. Figure 8 also shows the cumulative and total sums of $\Delta\chi^2$ for the NPs, with the sum for all NP of $\sum \Delta\chi^2 = -3.0$ corresponding to an approximate contribution to the signal significance of $\sqrt{|\sum \Delta\chi^2|} = 1.7\sigma$.

7 Summary

A first of its kind search for top squark pair production with subsequent decay characterized by two top quarks, additional gluons or light-flavor quarks, and low missing transverse momentum (p_T^{miss}) is described. Events containing exactly one electron or muon and at least seven jets, of which at least one should be b tagged, are selected from a sample of proton-proton collisions at $\sqrt{s} = 13$ TeV corresponding to an integrated luminosity of 137 fb^{-1} collected with the CMS detector in 2016–2018. No requirement is made on p_T^{miss} . The dominant $t\bar{t}$ background is predicted from data using a simultaneous fit of the jet multiplicity distribution across four bins of a neural network score.

The results are interpreted in terms of top squark pair production in the context of R -parity violating (RPV) and stealth supersymmetry models. Top squark masses ($m_{\tilde{t}}$) up to 670 GeV are excluded at 95% confidence level for the RPV model in which the top squark decays to a top

quark and the lightest neutralino, which subsequently decays to three light-flavor quarks via an off-shell squark through a trilinear coupling λ'' . Top squark masses up to 870 GeV are excluded for the stealth supersymmetry model in which the top squark decays to a top quark, three gluons, and a gravitino via intermediate hidden sector particles. The maximum observed local significance is 2.8 standard deviations corresponding to a best fit signal strength of 0.21 ± 0.07 for the RPV model with $m_{\tilde{\tau}} = 400$ GeV.

Acknowledgments

We congratulate our colleagues in the CERN accelerator departments for the excellent performance of the LHC and thank the technical and administrative staffs at CERN and at other CMS institutes for their contributions to the success of the CMS effort. In addition, we gratefully acknowledge the computing centers and personnel of the Worldwide LHC Computing Grid and other centers for delivering so effectively the computing infrastructure essential to our analyses. Finally, we acknowledge the enduring support for the construction and operation of the LHC, the CMS detector, and the supporting computing infrastructure provided by the following funding agencies: BMBWF and FWF (Austria); FNRS and FWO (Belgium); CNPq, CAPES, FAPERJ, FAPERGS, and FAPESP (Brazil); MES (Bulgaria); CERN; CAS, MoST, and NSFC (China); COLCIENCIAS (Colombia); MSES and CSF (Croatia); RIF (Cyprus); SENESCYT (Ecuador); MoER, ERC PUT and ERDF (Estonia); Academy of Finland, MEC, and HIP (Finland); CEA and CNRS/IN2P3 (France); BMBF, DFG, and HGF (Germany); GSRT (Greece); NK-FIA (Hungary); DAE and DST (India); IPM (Iran); SFI (Ireland); INFN (Italy); MSIP and NRF (Republic of Korea); MES (Latvia); LAS (Lithuania); MOE and UM (Malaysia); BUAP, CINVESTAV, CONACYT, LNS, SEP, and UASLP-FAI (Mexico); MOS (Montenegro); MBIE (New Zealand); PAEC (Pakistan); MSHE and NSC (Poland); FCT (Portugal); JINR (Dubna); MON, RosAtom, RAS, RFBR, and NRC KI (Russia); MESTD (Serbia); SEIDI, CPAN, PCTI, and FEDER (Spain); MOSTR (Sri Lanka); Swiss Funding Agencies (Switzerland); MST (Taipei); ThEPCenter, IPST, STAR, and NSTDA (Thailand); TUBITAK and TAEK (Turkey); NASU (Ukraine); STFC (United Kingdom); DOE and NSF (USA).

Individuals have received support from the Marie-Curie program and the European Research Council and Horizon 2020 Grant, contract Nos. 675440, 724704, 752730, and 765710 (European Union); the Leventis Foundation; the Alfred P. Sloan Foundation; the Alexander von Humboldt Foundation; the Belgian Federal Science Policy Office; the Fonds pour la Formation à la Recherche dans l'Industrie et dans l'Agriculture (FRIA-Belgium); the Agentschap voor Innovatie door Wetenschap en Technologie (IWT-Belgium); the F.R.S.-FNRS and FWO (Belgium) under the "Excellence of Science – EOS" – be.h project n. 30820817; the Beijing Municipal Science & Technology Commission, No. Z191100007219010; the Ministry of Education, Youth and Sports (MEYS) of the Czech Republic; the Deutsche Forschungsgemeinschaft (DFG), under Germany's Excellence Strategy – EXC 2121 "Quantum Universe" – 390833306, and under project number 400140256 - GRK2497; the Lendület ("Momentum") Program and the János Bolyai Research Scholarship of the Hungarian Academy of Sciences, the New National Excellence Program ÚNKP, the NKFI research grants 123842, 123959, 124845, 124850, 125105, 128713, 128786, and 129058 (Hungary); the Council of Science and Industrial Research, India; the HOMING PLUS program of the Foundation for Polish Science, cofinanced from European Union, Regional Development Fund, the Mobility Plus program of the Ministry of Science and Higher Education, the National Science Center (Poland), contracts Harmonia 2014/14/M/ST2/00428, Opus 2014/13/B/ST2/02543, 2014/15/B/ST2/03998, and 2015/19/B/ST2/02861, Sonata-bis 2012/07/E/ST2/01406; the National Priorities Research Program by Qatar National Research Fund; the Ministry of Science and Higher Education, project no. 0723-2020-0041 (Russia); the

Programa Estatal de Fomento de la Investigación Científica y Técnica de Excelencia María de Maeztu, grant MDM-2015-0509 and the Programa Severo Ochoa del Principado de Asturias; the Thalís and Aristeia programs cofinanced by EU-ESF and the Greek NSRF; the Rachadapisek Sompot Fund for Postdoctoral Fellowship, Chulalongkorn University and the Chulalongkorn Academic into Its 2nd Century Project Advancement Project (Thailand); the Kavli Foundation; the Nvidia Corporation; the SuperMicro Corporation; the Welch Foundation, contract C-1845; and the Weston Havens Foundation (USA).

References

- [1] P. Fayet and S. Ferrara, “Supersymmetry”, *Phys. Rept.* **32** (1977) 249, doi:10.1016/0370-1573(77)90066-7.
- [2] S. P. Martin, “A supersymmetry primer”, *Adv. Ser. Direct. High Energy Phys.* **21** (1997) 1, doi:10.1142/9789812839657_0001, arXiv:hep-ph/9709356.
- [3] S. Dimopoulos and G. F. Giudice, “Naturalness constraints in supersymmetric theories with nonuniversal soft terms”, *Phys. Lett. B* **357** (1995) 573, doi:10.1016/0370-2693(95)00961-J, arXiv:hep-ph/9507282.
- [4] R. Barbieri and G. F. Giudice, “Upper bounds on supersymmetric particle masses”, *Nucl. Phys. B* **306** (1988) 63, doi:10.1016/0550-3213(88)90171-X.
- [5] A. Pomarol and D. Tommasini, “Horizontal symmetries for the supersymmetric flavor problem”, *Nucl. Phys. B* **466** (1996) 3, doi:10.1016/0550-3213(96)00074-0, arXiv:hep-ph/9507462.
- [6] A. G. Cohen, D. B. Kaplan, and A. E. Nelson, “The more minimal supersymmetric standard model”, *Phys. Lett. B* **388** (1996) 588, doi:10.1016/S0370-2693(96)01183-5, arXiv:hep-ph/9607394.
- [7] M. Papucci, J. T. Ruderman, and A. Weiler, “Natural SUSY endures”, *JHEP* **09** (2012) 035, doi:10.1007/JHEP09(2012)035, arXiv:1110.6926.
- [8] C. Brust, A. Katz, S. Lawrence, and R. Sundrum, “SUSY, the third generation and the LHC”, *JHEP* **03** (2012) 103, doi:10.1007/JHEP03(2012)103, arXiv:1110.6670.
- [9] R. Barbier et al., “R-parity violating supersymmetry”, *Phys. Rept.* **420** (2005) 1, doi:10.1016/j.physrep.2005.08.006, arXiv:hep-ph/0406039.
- [10] D. S. M. Alves, E. Izaguirre, and J. G. Wacker, “Where the sidewalk ends: Jets and missing energy search strategies for the 7 TeV LHC”, *JHEP* **10** (2011) 012, doi:10.1007/JHEP10(2011)012, arXiv:1102.5338.
- [11] M. Lisanti, P. Schuster, M. Strassler, and N. Toro, “Study of LHC searches for a lepton and many jets”, *JHEP* **11** (2012) 081, doi:10.1007/JHEP11(2012)081, arXiv:1107.5055.
- [12] J. Fan, M. Reece, and J. T. Ruderman, “Stealth supersymmetry”, *JHEP* **11** (2011) 012, doi:10.1007/JHEP11(2011)012, arXiv:1105.5135.
- [13] G. F. Giudice and R. Rattazzi, “Theories with gauge mediated supersymmetry breaking”, *Phys. Rept.* **322** (1999) 419, doi:10.1016/S0370-1573(99)00042-3, arXiv:hep-ph/9801271.

- [14] S. P. Martin, “Compressed supersymmetry and natural neutralino dark matter from top squark-mediated annihilation to top quarks”, *Phys. Rev. D* **75** (2007) 115005, doi:10.1103/PhysRevD.75.115005, arXiv:hep-ph/0703097.
- [15] T. J. LeCompte and S. P. Martin, “Large Hadron Collider reach for supersymmetric models with compressed mass spectra”, *Phys. Rev. D* **84** (2011) 015004, doi:10.1103/PhysRevD.84.015004, arXiv:1105.4304.
- [16] M. J. Strassler, “Why unparticle models with mass gaps are examples of hidden valleys”, 2008. arXiv:0801.0629.
- [17] CMS Collaboration, “Search for supersymmetry in proton-proton collisions at 13 TeV using identified top quarks”, *Phys. Rev. D* **97** (2018) 012007, doi:10.1103/PhysRevD.97.012007, arXiv:1710.11188.
- [18] CMS Collaboration, “Search for direct production of supersymmetric partners of the top quark in the all-jets final state in proton-proton collisions at $\sqrt{s} = 13$ TeV”, *JHEP* **10** (2017) 005, doi:10.1007/JHEP10(2017)005, arXiv:1707.03316.
- [19] CMS Collaboration, “Search for top squark pair production in pp collisions at $\sqrt{s} = 13$ TeV using single lepton events”, *JHEP* **10** (2017) 019, doi:10.1007/JHEP10(2017)019, arXiv:1706.04402.
- [20] CMS Collaboration, “Search for top squarks and dark matter particles, in opposite-charge dilepton final states at $\sqrt{s} = 13$ TeV”, *Phys. Rev. D* **97** (2018) 032009, doi:10.1103/PhysRevD.97.032009, arXiv:1711.00752.
- [21] ATLAS Collaboration, “Search for a scalar partner of the top quark in the jets plus missing transverse momentum final state at $\sqrt{s} = 13$ TeV with the ATLAS detector”, *JHEP* **12** (2017) 085, doi:10.1007/JHEP12(2017)085, arXiv:1709.04183.
- [22] ATLAS Collaboration, “Search for top-squark pair production in final states with one lepton, jets, and missing transverse momentum using 36 fb^{-1} of $\sqrt{s} = 13$ TeV pp collision data with the ATLAS detector”, *JHEP* **06** (2018) 108, doi:10.1007/JHEP06(2018)108, arXiv:1711.11520.
- [23] J. Fan, M. Reece, and J. T. Ruderman, “A stealth supersymmetry sampler”, *JHEP* **07** (2012) 196, doi:10.1007/JHEP07(2012)196, arXiv:1201.4875.
- [24] J. Fan et al., “Stealth supersymmetry simplified”, *JHEP* **07** (2016) 016, doi:10.1007/JHEP07(2016)016, arXiv:1512.05781.
- [25] ATLAS Collaboration, “A search for pair-produced resonances in four-jet final states at $\sqrt{s} = 13$ TeV with the ATLAS detector”, *Eur. Phys. J. C* **78** (2018) 250, doi:10.1140/epjc/s10052-018-5693-4, arXiv:1710.07171.
- [26] CMS Collaboration, “Search for pair-produced resonances decaying to quark pairs in proton-proton collisions at $\sqrt{s} = 13$ TeV”, *Phys. Rev. D* **98** (2018) 112014, doi:10.1103/PhysRevD.98.112014, arXiv:1808.03124.
- [27] ATLAS Collaboration, “Search for B-L R -parity-violating top squarks in $\sqrt{s} = 13$ TeV pp collisions with the ATLAS experiment”, *Phys. Rev. D* **97** (2018) 032003, doi:10.1103/PhysRevD.97.032003, arXiv:1710.05544.

-
- [28] CMS Collaboration, “Search for pair production of third-generation scalar leptoquarks and top squarks in proton–proton collisions at $\sqrt{s} = 8$ TeV”, *Phys. Lett. B* **739** (2014) 229, doi:10.1016/j.physletb.2014.10.063, arXiv:1408.0806.
- [29] CMS Collaboration, “Search for R -parity violating decays of a top squark in proton-proton collisions at $\sqrt{s} = 8$ TeV”, *Phys. Lett. B* **760** (2016) 178, doi:10.1016/j.physletb.2016.06.039, arXiv:1602.04334.
- [30] ATLAS Collaboration, “Search for new phenomena in a lepton plus high jet multiplicity final state with the ATLAS experiment using $\sqrt{s} = 13$ TeV proton-proton collision data”, *JHEP* **09** (2017) 088, doi:10.1007/JHEP09(2017)088, arXiv:1704.08493.
- [31] CMS Collaboration, “Search for stealth supersymmetry in events with jets, either photons or leptons, and low missing transverse momentum in pp collisions at 8 TeV”, *Phys. Lett. B* **743** (2015) 503, doi:10.1016/j.physletb.2015.03.017, arXiv:1411.7255.
- [32] CMS Collaboration, “Search for supersymmetry in events with photons and low missing transverse energy in pp collisions at $\sqrt{s} = 7$ TeV”, *Phys. Lett. B* **719** (2013) 42, doi:10.1016/j.physletb.2012.12.055, arXiv:1210.2052.
- [33] J. A. Evans and Y. Kats, “LHC coverage of RPV MSSM with light stops”, *JHEP* **04** (2013) 028, doi:10.1007/JHEP04(2013)028, arXiv:1209.0764.
- [34] CMS Collaboration, “The CMS experiment at the CERN LHC”, *JINST* **3** (2008) S08004, doi:10.1088/1748-0221/3/08/S08004.
- [35] CMS Collaboration, “The CMS trigger system”, *JINST* **12** (2017) P01020, doi:10.1088/1748-0221/12/01/P01020, arXiv:1609.02366.
- [36] CMS Collaboration, “Particle-flow reconstruction and global event description with the CMS detector”, *JINST* **12** (2017) P10003, doi:10.1088/1748-0221/12/10/P10003, arXiv:1706.04965.
- [37] M. Cacciari, G. P. Salam, and G. Soyez, “The anti- k_T jet clustering algorithm”, *JHEP* **04** (2008) 063, doi:10.1088/1126-6708/2008/04/063, arXiv:0802.1189.
- [38] M. Cacciari, G. P. Salam, and G. Soyez, “FastJet user manual”, *Eur. Phys. J. C* **72** (2012) 1896, doi:10.1140/epjc/s10052-012-1896-2, arXiv:1111.6097.
- [39] CMS Collaboration, “Technical proposal for the Phase-II upgrade of the Compact Muon Solenoid”, CMS Technical Proposal CERN-LHCC-2015-010, CMS-TDR-15-02, CERN, 2015.
- [40] CMS Collaboration, “Performance of electron reconstruction and selection with the CMS detector in proton-proton collisions at $\sqrt{s} = 8$ TeV”, *JINST* **10** (2015) P06005, doi:10.1088/1748-0221/10/06/P06005, arXiv:1502.02701.
- [41] CMS Collaboration, “Performance of the CMS muon detector and muon reconstruction with proton-proton collisions at $\sqrt{s} = 13$ TeV”, *JINST* **13** (2018) P06015, doi:10.1088/1748-0221/13/06/P06015, arXiv:1804.04528.
- [42] K. Rehermann and B. Tweedie, “Efficient identification of boosted semileptonic top quarks at the LHC”, *JHEP* **03** (2011) 059, doi:10.1007/JHEP03(2011)059, arXiv:1007.2221.

- [43] CMS Collaboration, “Jet performance in pp collisions at 7 TeV”, CMS Physics Analysis Summary CMS-PAS-JME-10-003, 2010.
- [44] CMS Collaboration, “Jet algorithms performance in 13 TeV data”, CMS Physics Analysis Summary CMS-PAS-JME-16-003, 2017.
- [45] CMS Collaboration, “Jet energy scale and resolution in the CMS experiment in pp collisions at 8 TeV”, *JINST* **12** (2017) P02014, doi:10.1088/1748-0221/12/02/P02014, arXiv:1607.03663.
- [46] CMS Collaboration, “Jet energy scale and resolution performance with 13 TeV data collected by CMS in 2016–2018”, CMS Detector Performance Note CMS-DP-2020-019, 2020.
- [47] M. Cacciari and G. P. Salam, “Pileup subtraction using jet areas”, *Phys. Lett. B* **659** (2008) 119, doi:10.1016/j.physletb.2007.09.077, arXiv:0707.1378.
- [48] CMS Collaboration, “Identification of heavy-flavour jets with the CMS detector in pp collisions at 13 TeV”, *JINST* **13** (2018) P05011, doi:10.1088/1748-0221/13/05/P05011, arXiv:1712.07158.
- [49] P. Nason, “A new method for combining NLO QCD with shower Monte Carlo algorithms”, *JHEP* **11** (2004) 040, doi:10.1088/1126-6708/2004/11/040, arXiv:hep-ph/0409146.
- [50] S. Frixione, P. Nason, and C. Oleari, “Matching NLO QCD computations with parton shower simulations: the POWHEG method”, *JHEP* **11** (2007) 070, doi:10.1088/1126-6708/2007/11/070, arXiv:0709.2092.
- [51] S. Alioli, P. Nason, C. Oleari, and E. Re, “A general framework for implementing NLO calculations in shower Monte Carlo programs: the POWHEG box”, *JHEP* **06** (2010) 043, doi:10.1007/JHEP06(2010)043, arXiv:1002.2581.
- [52] S. Frixione, P. Nason, and G. Ridolfi, “A positive-weight next-to-leading-order Monte Carlo for heavy flavour hadroproduction”, *JHEP* **09** (2007) 126, doi:10.1088/1126-6708/2007/09/126, arXiv:0707.3088.
- [53] R. Frederix, E. Re, and P. Torrielli, “Single-top t -channel hadroproduction in the four-flavour scheme with POWHEG and amc@nlo”, *JHEP* **09** (2012) 130, doi:10.1007/JHEP09(2012)130, arXiv:1207.5391.
- [54] J. Alwall et al., “The automated computation of tree-level and next-to-leading order differential cross sections, and their matching to parton shower simulations”, *JHEP* **07** (2014) 079, doi:10.1007/JHEP07(2014)079, arXiv:1405.0301.
- [55] A. Kalogeropoulos and J. Alwall, “The SysCalc code: A tool to derive theoretical systematic uncertainties”, 2018. arXiv:1801.08401.
- [56] T. Sjöstrand et al., “An introduction to PYTHIA 8.2”, *Comput. Phys. Commun.* **191** (2015) 159, doi:10.1016/j.cpc.2015.01.024, arXiv:1410.3012.
- [57] C. Borschensky et al., “Squark and gluino production cross sections in pp collisions at $\sqrt{s} = 13, 14, 33$ and 100 TeV”, *Eur. Phys. J. C* **74** (2014) 3174, doi:10.1140/epjc/s10052-014-3174-y, arXiv:1407.5066.

-
- [58] W. Beenakker et al., “NNLL-fast: predictions for coloured supersymmetric particle production at the LHC with threshold and Coulomb resummation”, *JHEP* **12** (2016) 133, doi:10.1007/JHEP12(2016)133, arXiv:1607.07741.
- [59] NNPDF Collaboration, “Parton distributions for the LHC Run II”, *JHEP* **04** (2015) 040, doi:10.1007/JHEP04(2015)040, arXiv:1410.8849.
- [60] NNPDF Collaboration, “Parton distributions from high-precision collider data”, *Eur. Phys. J. C* **77** (2017) 663, doi:10.1140/epjc/s10052-017-5199-5, arXiv:1706.00428.
- [61] CMS Collaboration, “Event generator tunes obtained from underlying event and multiparton scattering measurements”, *Eur. Phys. J. C* **76** (2016) 155, doi:10.1140/epjc/s10052-016-3988-x, arXiv:1512.00815.
- [62] CMS Collaboration, “Investigations of the impact of the parton shower tuning in PYTHIA 8 in the modelling of $t\bar{t}$ at $\sqrt{s} = 8$ and 13 TeV”, CMS Physics Analysis Summary CMS-PAS-TOP-16-021, 2016.
- [63] CMS Collaboration, “Extraction and validation of a new set of CMS PYTHIA 8 tunes from underlying-event measurements”, *Eur. Phys. J. C* **80** (2020) 4, doi:10.1140/epjc/s10052-019-7499-4, arXiv:1903.12179.
- [64] GEANT4 Collaboration, “GEANT4—a simulation toolkit”, *Nucl. Instrum. Meth. A* **506** (2003) 250, doi:10.1016/S0168-9002(03)01368-8.
- [65] M. Czakon and A. Mitov, “Top++: A program for the calculation of the top-pair cross-section at hadron colliders”, *Comput. Phys. Commun.* **185** (2014) 2930, doi:10.1016/j.cpc.2014.06.021, arXiv:1112.5675.
- [66] P. Kant et al., “HATHOR for single top-quark production: Updated predictions and uncertainty estimates for single top-quark production in hadronic collisions”, *Comput. Phys. Commun.* **191** (2015) 74, doi:10.1016/j.cpc.2015.02.001, arXiv:1406.4403.
- [67] M. Aliev et al., “HATHOR: HAdronic Top and Heavy quarks crOss section calculatoR”, *Comput. Phys. Commun.* **182** (2011) 1034, doi:10.1016/j.cpc.2010.12.040, arXiv:1007.1327.
- [68] T. Gehrmann et al., “ W^+W^- production at hadron colliders in next to next to leading order QCD”, *Phys. Rev. Lett.* **113** (2014) 212001, doi:10.1103/PhysRevLett.113.212001, arXiv:1408.5243.
- [69] J. M. Campbell and R. K. Ellis, “An update on vector boson pair production at hadron colliders”, *Phys. Rev. D* **60** (1999) 113006, doi:10.1103/PhysRevD.60.113006, arXiv:hep-ph/9905386.
- [70] J. M. Campbell, R. K. Ellis, and C. Williams, “Vector boson pair production at the LHC”, *JHEP* **07** (2011) 018, doi:10.1007/JHEP07(2011)018, arXiv:1105.0020.
- [71] Y. Li and F. Petriello, “Combining QCD and electroweak corrections to dilepton production in FEWZ”, *Phys. Rev. D* **86** (2012) 094034, doi:10.1103/PhysRevD.86.094034, arXiv:1208.5967.

- [72] Y. Ganin and V. Lempitsky, “Unsupervised domain adaptation by backpropagation”, 2014. arXiv:1409.7495.
- [73] G. C. Fox and S. Wolfram, “Observables for the analysis of event shapes in $e^+ e^-$ annihilation and other processes”, *Phys. Rev. Lett.* **41** (1978) 1581, doi:10.1103/PhysRevLett.41.1581.
- [74] J. D. Bjorken and S. J. Brodsky, “Statistical model for electron-positron annihilation into hadrons”, *Phys. Rev. D* **1** (1970) 1416, doi:10.1103/PhysRevD.1.1416.
- [75] E. Gerwick, T. Plehn, S. Schumann, and P. Schichtel, “Scaling patterns for QCD jets”, *JHEP* **10** (2012) 162, doi:10.1007/JHEP10(2012)162, arXiv:1208.3676.
- [76] M. Cacciari et al., “The $t\bar{t}$ cross-section at 1.8 TeV and 1.96 TeV: A study of the systematics due to parton densities and scale dependence”, *JHEP* **04** (2004) 068, doi:10.1088/1126-6708/2004/04/068, arXiv:hep-ph/0303085.
- [77] S. Catani, D. de Florian, M. Grazzini, and P. Nason, “Soft gluon resummation for Higgs boson production at hadron colliders”, *JHEP* **07** (2003) 028, doi:10.1088/1126-6708/2003/07/028, arXiv:hep-ph/0306211.
- [78] CMS Collaboration, “Measurement of the inelastic proton-proton cross section at $\sqrt{s} = 13$ TeV”, *JHEP* **07** (2018) 161, doi:10.1007/JHEP07(2018)161, arXiv:1802.02613.
- [79] CMS Collaboration, “CMS luminosity measurements for the 2016 data taking period”, CMS Physics Analysis Summary CMS-PAS-LUM-17-001, 2017.
- [80] CMS Collaboration, “CMS luminosity measurements for the 2017 data taking period at $\sqrt{s} = 13$ TeV”, CMS Physics Analysis Summary CMS-PAS-LUM-17-004, 2017.
- [81] CMS Collaboration, “CMS luminosity measurements for the 2018 data taking period at $\sqrt{s} = 13$ TeV”, CMS Physics Analysis Summary CMS-PAS-LUM-18-002, 2018.
- [82] L. Demortier, “ p -values and nuisance parameters”, in *Statistical issues for LHC physics. Proceedings, Workshop, PHYSTAT-LHC, Geneva, Switzerland, June 27-29, 2007*, p. 23. 2008. doi:10.5170/CERN-2008-001.
- [83] ATLAS and CMS Collaborations, The LHC Higgs Combination Group, “Procedure for the LHC Higgs boson search combination in Summer 2011”, Technical Report CMS-NOTE-2011-005, ATL-PHYS-PUB-2011-11, 2011.
- [84] T. Junk, “Confidence level computation for combining searches with small statistics”, *Nucl. Instrum. Meth. A* **434** (1999) 435, doi:10.1016/S0168-9002(99)00498-2, arXiv:hep-ex/9902006.
- [85] A. L. Read, “Presentation of search results: The CL_s technique”, *J. Phys. G* **28** (2002) 2693, doi:10.1088/0954-3899/28/10/313.
- [86] G. Cowan, K. Cranmer, E. Gross, and O. Vitells, “Asymptotic formulae for likelihood-based tests of new physics”, *Eur. Phys. J. C* **71** (2011) 1554, doi:10.1140/epjc/s10052-011-1554-0, arXiv:1007.1727. [Erratum: doi:10.1140/epjc/s10052-013-2501-z].

A The CMS Collaboration

Yerevan Physics Institute, Yerevan, Armenia

A.M. Sirunyan[†], A. Tumasyan

Institut für Hochenergiephysik, Wien, Austria

W. Adam, J.W. Andrejkovic, T. Bergauer, S. Chatterjee, M. Dragicevic, A. Escalante Del Valle, R. Frühwirth¹, M. Jeitler¹, N. Krammer, L. Lechner, D. Liko, I. Mikulec, F.M. Pitters, J. Schieck¹, R. Schöfbeck, M. Spanring, S. Templ, W. Waltenberger, C.-E. Wulz¹

Institute for Nuclear Problems, Minsk, Belarus

V. Chekhovsky, A. Litomin, V. Makarenko

Universiteit Antwerpen, Antwerpen, Belgium

M.R. Darwish², E.A. De Wolf, X. Janssen, T. Kello³, A. Lelek, H. Rejeb Sfar, P. Van Mechelen, S. Van Putte, N. Van Remortel

Vrije Universiteit Brussel, Brussel, Belgium

F. Blekman, E.S. Bols, J. D'Hondt, J. De Clercq, M. Delcourt, S. Lowette, S. Moortgat, A. Morton, D. Müller, A.R. Sahasransu, S. Tavernier, W. Van Doninck, P. Van Mulders

Université Libre de Bruxelles, Bruxelles, Belgium

D. Beghin, B. Bilin, B. Clerbaux, G. De Lentdecker, L. Favart, A. Grebenyuk, A.K. Kalsi, K. Lee, M. Mahdavihorrani, I. Makarenko, L. Moureaux, L. Pétré, A. Popov, N. Postiau, E. Starling, L. Thomas, M. Vanden Bemden, C. Vander Velde, P. Vanlaer, D. Vannerom, L. Wezenbeek

Ghent University, Ghent, Belgium

T. Cornelis, D. Dobur, M. Gruchala, G. Mestdach, M. Niedziela, C. Roskas, K. Skovpen, M. Tytgat, W. Verbeke, B. Vermassen, M. Vit

Université Catholique de Louvain, Louvain-la-Neuve, Belgium

A. Bethani, G. Bruno, F. Bury, C. Caputo, P. David, C. Delaere, I.S. Donertas, A. Giammanco, V. Lemaitre, K. Mondal, J. Prisciandaro, A. Taliencio, M. Teklishyn, P. Vischia, S. Wertz, S. Wuyckens

Centro Brasileiro de Pesquisas Fisicas, Rio de Janeiro, Brazil

G.A. Alves, C. Hensel, A. Moraes

Universidade do Estado do Rio de Janeiro, Rio de Janeiro, Brazil

W.L. Aldá Júnior, M. Barroso Ferreira Filho, H. Brandao Malbouisson, W. Carvalho, J. Chinellato⁴, E.M. Da Costa, G.G. Da Silveira⁵, D. De Jesus Damiao, S. Fonseca De Souza, D. Matos Figueiredo, C. Mora Herrera, K. Mota Amarilo, L. Mundim, H. Nogima, P. Rebello Teles, L.J. Sanchez Rosas, A. Santoro, S.M. Silva Do Amaral, A. Sznajder, M. Thiel, F. Torres Da Silva De Araujo, A. Vilela Pereira

Universidade Estadual Paulista ^a, Universidade Federal do ABC ^b, São Paulo, Brazil

C.A. Bernardes^{a,a}, L. Calligaris^a, T.R. Fernandez Perez Tomei^a, E.M. Gregores^{a,b}, D.S. Lemos^a, P.G. Mercadante^{a,b}, S.F. Novaes^a, Sandra S. Padula^a

Institute for Nuclear Research and Nuclear Energy, Bulgarian Academy of Sciences, Sofia, Bulgaria

A. Aleksandrov, G. Antchev, I. Atanasov, R. Hadjiiska, P. Iaydjiev, M. Misheva, M. Rodozov, M. Shopova, G. Sultanov

University of Sofia, Sofia, Bulgaria

A. Dimitrov, T. Ivanov, L. Litov, B. Pavlov, P. Petkov, A. Petrov

Beihang University, Beijing, China

T. Cheng, W. Fang³, Q. Guo, T. Javaid⁶, M. Mittal, H. Wang, L. Yuan

Department of Physics, Tsinghua University, Beijing, China

M. Ahmad, G. Bauer, C. Dozen⁷, Z. Hu, J. Martins⁸, Y. Wang, K. Yi^{9,10}

Institute of High Energy Physics, Beijing, China

E. Chapon, G.M. Chen⁶, H.S. Chen⁶, M. Chen, A. Kapoor, D. Leggat, H. Liao, Z.-A. LIU⁶, R. Sharma, A. Spiezia, J. Tao, J. Thomas-wilsker, J. Wang, H. Zhang, S. Zhang⁶, J. Zhao

State Key Laboratory of Nuclear Physics and Technology, Peking University, Beijing, China

A. Agapitos, Y. Ban, C. Chen, Q. Huang, A. Levin, Q. Li, M. Lu, X. Lyu, Y. Mao, S.J. Qian, D. Wang, Q. Wang, J. Xiao

Sun Yat-Sen University, Guangzhou, China

Z. You

Institute of Modern Physics and Key Laboratory of Nuclear Physics and Ion-beam Application (MOE) - Fudan University, Shanghai, China

X. Gao³, H. Okawa

Zhejiang University, Hangzhou, China

M. Xiao

Universidad de Los Andes, Bogota, Colombia

C. Avila, A. Cabrera, C. Florez, J. Fraga, A. Sarkar, M.A. Segura Delgado

Universidad de Antioquia, Medellin, Colombia

J. Jaramillo, J. Mejia Guisao, F. Ramirez, J.D. Ruiz Alvarez, C.A. Salazar González, N. Vanegas Arbelaez

University of Split, Faculty of Electrical Engineering, Mechanical Engineering and Naval Architecture, Split, Croatia

D. Giljanovic, N. Godinovic, D. Lelas, I. Puljak

University of Split, Faculty of Science, Split, Croatia

Z. Antunovic, M. Kovac, T. Sculac

Institute Rudjer Boskovic, Zagreb, Croatia

V. Brigljevic, D. Ferencek, D. Majumder, M. Roguljic, A. Starodumov¹¹, T. Susa

University of Cyprus, Nicosia, Cyprus

A. Attikis, E. Erodotou, A. Ioannou, G. Kole, M. Kolosova, S. Konstantinou, J. Mousa, C. Nicolaou, F. Ptochos, P.A. Razis, H. Rykaczewski, H. Saka

Charles University, Prague, Czech Republic

M. Finger¹², M. Finger Jr.¹², A. Kveton

Escuela Politecnica Nacional, Quito, Ecuador

E. Ayala

Universidad San Francisco de Quito, Quito, Ecuador

E. Carrera Jarrin

Academy of Scientific Research and Technology of the Arab Republic of Egypt, Egyptian Network of High Energy Physics, Cairo, Egypt

S. Abu Zeid¹³, S. Khalil¹⁴, E. Salama^{15,13}

Center for High Energy Physics (CHEP-FU), Fayoum University, El-Fayoum, Egypt

A. Lotfy, Y. Mohammed

National Institute of Chemical Physics and Biophysics, Tallinn, Estonia

S. Bhowmik, A. Carvalho Antunes De Oliveira, R.K. Dewanjee, K. Ehataht, M. Kadastik, J. Pata, M. Raidal, C. Veelken

Department of Physics, University of Helsinki, Helsinki, Finland

P. Eerola, L. Forthomme, H. Kirschenmann, K. Osterberg, M. Voutilainen

Helsinki Institute of Physics, Helsinki, Finland

E. Brücken, F. Garcia, J. Havukainen, V. Karimäki, M.S. Kim, R. Kinnunen, T. Lampén, K. Lassila-Perini, S. Lehti, T. Lindén, H. Siikonen, E. Tuominen, J. Tuominiemi

Lappeenranta University of Technology, Lappeenranta, Finland

P. Luukka, H. Petrow, T. Tuuva

IRFU, CEA, Université Paris-Saclay, Gif-sur-Yvette, France

C. Amendola, M. Besancon, F. Couderc, M. Dejardin, D. Denegri, J.L. Faure, F. Ferri, S. Ganjour, A. Givernaud, P. Gras, G. Hamel de Monchenault, P. Jarry, B. Lenzi, E. Locci, J. Malcles, J. Rander, A. Rosowsky, M.Ö. Sahin, A. Savoy-Navarro¹⁶, M. Titov, G.B. Yu

Laboratoire Leprince-Ringuet, CNRS/IN2P3, Ecole Polytechnique, Institut Polytechnique de Paris, Palaiseau, France

S. Ahuja, F. Beaudette, M. Bonanomi, A. Buchot Perraguin, P. Busson, C. Charlot, O. Davignon, B. Diab, G. Falmagne, S. Ghosh, R. Granier de Cassagnac, A. Hakimi, I. Kucher, A. Lobanov, M. Nguyen, C. Ochando, P. Paganini, J. Rembser, R. Salerno, J.B. Sauvan, Y. Sirois, A. Zabi, A. Zghiche

Université de Strasbourg, CNRS, IPHC UMR 7178, Strasbourg, France

J.-L. Agram¹⁷, J. Andrea, D. Apparú, D. Bloch, G. Bourgatte, J.-M. Brom, E.C. Chabert, C. Collard, D. Darej, J.-C. Fontaine¹⁷, U. Goerlach, C. Grimault, A.-C. Le Bihan, P. Van Hove

Institut de Physique des 2 Infinis de Lyon (IP2I), Villeurbanne, France

E. Asilar, S. Beauceron, C. Bernet, G. Boudoul, C. Camen, A. Carle, N. Chanon, D. Contardo, P. Depasse, H. El Mamouni, J. Fay, S. Gascon, M. Gouzevitch, B. Ille, Sa. Jain, I.B. Laktineh, H. Lattaud, A. Lesauvage, M. Lethuillier, L. Mirabito, K. Shchablo, L. Torterotot, G. Touquet, M. Vander Donckt, S. Viret

Georgian Technical University, Tbilisi, Georgia

G. Adamov, Z. Tsamalaidze¹²

RWTH Aachen University, I. Physikalisches Institut, Aachen, Germany

L. Feld, K. Klein, M. Lipinski, D. Meuser, A. Pauls, M.P. Rauch, J. Schulz, M. Teroerde

RWTH Aachen University, III. Physikalisches Institut A, Aachen, Germany

D. Eliseev, M. Erdmann, P. Fackeldey, B. Fischer, S. Ghosh, T. Hebbeker, K. Hoepfner, H. Keller, L. Mastrolorenzo, M. Merschmeyer, A. Meyer, G. Mocellin, S. Mondal, S. Mukherjee, D. Noll, A. Novak, T. Pook, A. Pozdnyakov, Y. Rath, H. Reithler, J. Roemer, A. Schmidt, S.C. Schuler, A. Sharma, S. Wiedenbeck, S. Zaleski

RWTH Aachen University, III. Physikalisches Institut B, Aachen, Germany

C. Dziwok, G. Flügge, W. Haj Ahmad¹⁸, O. Hlushchenko, T. Kress, A. Nowack, C. Pistone, O. Pooth, D. Roy, H. Sert, A. Stahl¹⁹, T. Ziemons

Deutsches Elektronen-Synchrotron, Hamburg, Germany

H. Aarup Petersen, M. Aldaya Martin, P. Asmuss, I. Babounikau, S. Baxter, O. Behnke, A. Bermúdez Martínez, A.A. Bin Anuar, K. Borras²⁰, V. Botta, D. Brunner, A. Campbell, A. Cardini, P. Connor, S. Consuegra Rodríguez, V. Danilov, M.M. Defranchis, L. Didukh, D. Domínguez Damiani, G. Eckerlin, D. Eckstein, L.I. Estevez Banos, E. Gallo²¹, A. Geiser, A. Giraldi, A. Grohsjean, M. Guthoff, A. Harb, A. Jafari²², N.Z. Jomhari, H. Jung, A. Kasem²⁰, M. Kasemann, H. Kaveh, C. Kleinwort, J. Knolle, D. Krücker, W. Lange, T. Lenz, J. Lidrych, K. Lipka, W. Lohmann²³, T. Madlener, R. Mankel, I.-A. Melzer-Pellmann, J. Metwally, A.B. Meyer, M. Meyer, J. Mnich, A. Mussgiller, V. Myronenko, Y. Otariid, D. Pérez Adán, S.K. Pflitsch, D. Pitzl, A. Raspereza, A. Saggio, A. Saibel, M. Savitskyi, V. Scheurer, C. Schwanenberger, A. Singh, R.E. Sosa Ricardo, N. Tonon, O. Turkot, A. Vagnerini, M. Van De Klundert, R. Walsh, D. Walter, Y. Wen, K. Wichmann, C. Wissing, S. Wuchterl, O. Zenaiev, R. Zlebcik

University of Hamburg, Hamburg, Germany

R. Aggleton, S. Bein, L. Benato, A. Benecke, K. De Leo, T. Dreyer, M. Eich, F. Feindt, A. Fröhlich, C. Garbers, E. Garutti, P. Gunnellini, J. Haller, A. Hinzmann, A. Karavdina, G. Kasieczka, R. Klanner, R. Kogler, V. Kutzner, J. Lange, T. Lange, A. Malara, A. Nigamova, K.J. Pena Rodriguez, O. Rieger, P. Schleper, M. Schröder, J. Schwandt, D. Schwarz, J. Sonneveld, H. Stadie, G. Steinbrück, A. Tews, B. Vormwald, I. Zoi

Karlsruher Institut fuer Technologie, Karlsruhe, Germany

J. Bechtel, T. Berger, E. Butz, R. Caspart, T. Chwalek, W. De Boer, A. Dierlamm, A. Droll, K. El Morabit, N. Faltermann, K. Flöh, M. Giffels, J.o. Gosewisch, A. Gottmann, F. Hartmann¹⁹, C. Heidecker, U. Husemann, I. Katkov²⁴, P. Keicher, R. Koppenhöfer, S. Maier, M. Metzler, S. Mitra, Th. Müller, M. Musich, M. Neukum, G. Quast, K. Rabbertz, J. Rauser, D. Savoiiu, D. Schäfer, M. Schnepf, D. Seith, I. Shvetsov, H.J. Simonis, R. Ulrich, J. Van Der Linden, R.F. Von Cube, M. Wassmer, M. Weber, S. Wieland, R. Wolf, S. Wozniewski, S. Wunsch

Institute of Nuclear and Particle Physics (INPP), NCSR Demokritos, Aghia Paraskevi, Greece

G. Anagnostou, P. Asenov, G. Daskalakis, T. Geralis, A. Kyriakis, D. Loukas, A. Stakia

National and Kapodistrian University of Athens, Athens, Greece

M. Diamantopoulou, D. Karasavvas, G. Karathanasis, P. Kontaxakis, C.K. Koraka, A. Manousakis-katsikakis, A. Panagiotou, I. Papavergou, N. Saoulidou, K. Theofilatos, E. Tziaferi, K. Vellidis, E. Vourliotis

National Technical University of Athens, Athens, Greece

G. Bakas, K. Kousouris, I. Papakrivopoulos, G. Tsipolitis, A. Zacharopoulou

University of Ioánnina, Ioánnina, Greece

I. Evangelou, C. Foudas, P. Giannelis, P. Katsoulis, P. Kokkas, N. Manthos, I. Papadopoulos, J. Strologas

MTA-ELTE Lendület CMS Particle and Nuclear Physics Group, Eötvös Loránd University, Budapest, Hungary

M. Csanad, M.M.A. Gadallah²⁵, S. Lökös²⁶, P. Major, K. Mandal, A. Mehta, G. Pasztor, A.J. Rádl, O. Surányi, G.I. Veres

Wigner Research Centre for Physics, Budapest, Hungary

M. Bartók²⁷, G. Bencze, C. Hajdu, D. Horvath²⁸, F. Sikler, V. Veszpremi, G. Vesztergombi[†]

Institute of Nuclear Research ATOMKI, Debrecen, HungaryS. Czellar, J. Karancsi²⁷, J. Molnar, Z. Szillasi, D. Teyssier**Institute of Physics, University of Debrecen, Debrecen, Hungary**P. Raics, Z.L. Trocsanyi²⁹, B. Ujvari**Eszterhazy Karoly University, Karoly Robert Campus, Gyongyos, Hungary**T. Csorgo³⁰, F. Nemes³⁰, T. Novak**Indian Institute of Science (IISc), Bangalore, India**

S. Choudhury, J.R. Komaragiri, D. Kumar, L. Panwar, P.C. Tiwari

National Institute of Science Education and Research, HBNI, Bhubaneswar, IndiaS. Bahinipati³¹, D. Dash, C. Kar, P. Mal, T. Mishra, V.K. Muraleedharan Nair Bindhu³², A. Nayak³², P. Saha, N. Sur, S.K. Swain**Panjab University, Chandigarh, India**S. Bansal, S.B. Beri, V. Bhatnagar, G. Chaudhary, S. Chauhan, N. Dhingra³³, R. Gupta, A. Kaur, S. Kaur, P. Kumari, M. Meena, K. Sandeep, J.B. Singh, A.K. Viridi**University of Delhi, Delhi, India**

A. Ahmed, A. Bhardwaj, B.C. Choudhary, R.B. Garg, M. Gola, S. Keshri, A. Kumar, M. Naimuddin, P. Priyanka, K. Ranjan, A. Shah

Saha Institute of Nuclear Physics, HBNI, Kolkata, IndiaM. Bharti³⁴, R. Bhattacharya, S. Bhattacharya, D. Bhowmik, S. Dutta, B. Gomber³⁵, M. Maity³⁶, S. Nandan, P. Palit, P.K. Rout, G. Saha, B. Sahu, S. Sarkar, M. Sharan, B. Singh³⁴, S. Thakur³⁴**Indian Institute of Technology Madras, Madras, India**

P.K. Behera, S.C. Behera, P. Kalbhor, A. Muhammad, R. Pradhan, P.R. Pujahari, A. Sharma, A.K. Sikdar

Bhabha Atomic Research Centre, Mumbai, IndiaD. Dutta, V. Jha, V. Kumar, D.K. Mishra, K. Naskar³⁷, P.K. Netrakanti, L.M. Pant, P. Shukla**Tata Institute of Fundamental Research-A, Mumbai, India**

T. Aziz, S. Dugad, G.B. Mohanty, U. Sarkar

Tata Institute of Fundamental Research-B, Mumbai, India

S. Banerjee, S. Bhattacharya, R. Chudasama, M. Guchait, S. Karmakar, S. Kumar, G. Majumder, K. Mazumdar, S. Mukherjee, D. Roy

Indian Institute of Science Education and Research (IISER), Pune, India

S. Dube, B. Kansal, S. Pandey, A. Rane, A. Rastogi, S. Sharma

Department of Physics, Isfahan University of Technology, Isfahan, IranH. Bakhshiansohi³⁸, M. Zeinali³⁹**Institute for Research in Fundamental Sciences (IPM), Tehran, Iran**S. Chenarani⁴⁰, S.M. Etesami, M. Khakzad, M. Mohammadi Najafabadi**University College Dublin, Dublin, Ireland**

M. Felcini, M. Grunewald

INFN Sezione di Bari ^a, Università di Bari ^b, Politecnico di Bari ^c, Bari, ItalyM. Abbrescia^{a,b}, R. Aly^{a,b,41}, C. Aruta^{a,b}, A. Colaleo^a, D. Creanza^{a,c}, N. De Filippis^{a,c}, M. De Palma^{a,b}, A. Di Florio^{a,b}, A. Di Pilato^{a,b}, W. Elmetenawee^{a,b}, L. Fiore^a, A. Gelmi^{a,b},

M. Gul^a, G. Iaselli^{a,c}, M. Ince^{a,b}, S. Lezki^{a,b}, G. Maggi^{a,c}, M. Maggi^a, I. Margjeka^{a,b}, V. Mastrapasqua^{a,b}, J.A. Merlin^a, S. My^{a,b}, S. Nuzzo^{a,b}, A. Pompili^{a,b}, G. Pugliese^{a,c}, A. Ranieri^a, G. Selvaggi^{a,b}, L. Silvestris^a, F.M. Simone^{a,b}, R. Venditti^a, P. Verwilligen^a

INFN Sezione di Bologna ^a, Università di Bologna ^b, Bologna, Italy

G. Abbiendi^a, C. Battilana^{a,b}, D. Bonacorsi^{a,b}, L. Borgonovi^a, S. Braibant-Giacomelli^{a,b}, L. Brigliadori^a, R. Campanini^{a,b}, P. Capiluppi^{a,b}, A. Castro^{a,b}, F.R. Cavallo^a, C. Ciocca^a, M. Cuffiani^{a,b}, G.M. Dallavalle^a, T. Diotallevi^{a,b}, F. Fabbri^a, A. Fanfani^{a,b}, E. Fontanesi^{a,b}, P. Giacomelli^a, L. Giommi^{a,b}, C. Grandi^a, L. Guiducci^{a,b}, F. Iemmi^{a,b}, S. Lo Meo^{a,42}, S. Marcellini^a, G. Masetti^a, F.L. Navarria^{a,b}, A. Perrotta^a, F. Primavera^{a,b}, A.M. Rossi^{a,b}, T. Rovelli^{a,b}, G.P. Siroli^{a,b}, N. Tosi^a

INFN Sezione di Catania ^a, Università di Catania ^b, Catania, Italy

S. Albergo^{a,b,43}, S. Costa^{a,b,43}, A. Di Mattia^a, R. Potenza^{a,b}, A. Tricomi^{a,b,43}, C. Tuve^{a,b}

INFN Sezione di Firenze ^a, Università di Firenze ^b, Firenze, Italy

G. Barbagli^a, A. Cassese^a, R. Ceccarelli^{a,b}, V. Ciulli^{a,b}, C. Civinini^a, R. D'Alessandro^{a,b}, F. Fiori^{a,b}, E. Focardi^{a,b}, G. Latino^{a,b}, P. Lenzi^{a,b}, M. Lizzo^{a,b}, M. Meschini^a, S. Paoletti^a, R. Seidita^{a,b}, G. Sguazzoni^a, L. Viliani^a

INFN Laboratori Nazionali di Frascati, Frascati, Italy

L. Benussi, S. Bianco, D. Piccolo

INFN Sezione di Genova ^a, Università di Genova ^b, Genova, Italy

M. Bozzo^{a,b}, F. Ferro^a, R. Mulargia^{a,b}, E. Robutti^a, S. Tosi^{a,b}

INFN Sezione di Milano-Bicocca ^a, Università di Milano-Bicocca ^b, Milano, Italy

A. Benaglia^a, F. Brivio^{a,b}, F. Cetorelli^{a,b}, V. Ciriolo^{a,b,19}, F. De Guio^{a,b}, M.E. Dinardo^{a,b}, P. Dini^a, S. Gennai^a, A. Ghezzi^{a,b}, P. Govoni^{a,b}, L. Guzzi^{a,b}, M. Malberti^a, S. Malvezzi^a, A. Massironi^a, D. Menasce^a, F. Monti^{a,b}, L. Moroni^a, M. Paganoni^{a,b}, D. Pedrini^a, S. Ragazzi^{a,b}, T. Tabarelli de Fatis^{a,b}, D. Valsecchi^{a,b,19}, D. Zuolo^{a,b}

INFN Sezione di Napoli ^a, Università di Napoli 'Federico II' ^b, Napoli, Italy, Università della Basilicata ^c, Potenza, Italy, Università G. Marconi ^d, Roma, Italy

S. Buontempo^a, F. Carnevali^{a,b}, N. Cavallo^{a,c}, A. De Iorio^{a,b}, F. Fabozzi^{a,c}, A.O.M. Iorio^{a,b}, L. Lista^{a,b}, S. Meola^{a,d,19}, P. Paolucci^{a,19}, B. Rossi^a, C. Sciacca^{a,b}

INFN Sezione di Padova ^a, Università di Padova ^b, Padova, Italy, Università di Trento ^c, Trento, Italy

P. Azzi^a, N. Bacchetta^a, D. Bisello^{a,b}, P. Bortignon^a, A. Bragagnolo^{a,b}, R. Carlin^{a,b}, P. Checchia^a, P. De Castro Manzano^a, T. Dorigo^a, F. Gasparini^{a,b}, U. Gasparini^{a,b}, S.Y. Hoh^{a,b}, L. Layer^{a,44}, M. Margoni^{a,b}, A.T. Meneguzzo^{a,b}, M. Presilla^{a,b}, P. Ronchese^{a,b}, R. Rossin^{a,b}, F. Simonetto^{a,b}, G. Strong^a, M. Tosi^{a,b}, H. YARAR^{a,b}, M. Zanetti^{a,b}, P. Zotto^{a,b}, A. Zucchetta^{a,b}, G. Zumerle^{a,b}

INFN Sezione di Pavia ^a, Università di Pavia ^b, Pavia, Italy

C. Aime^{a,b}, A. Braghieri^a, S. Calzaferri^{a,b}, D. Fiorina^{a,b}, P. Montagna^{a,b}, S.P. Ratti^{a,b}, V. Re^a, M. Ressegotti^{a,b}, C. Riccardi^{a,b}, P. Salvini^a, I. Vai^a, P. Vitulo^{a,b}

INFN Sezione di Perugia ^a, Università di Perugia ^b, Perugia, Italy

G.M. Bilei^a, D. Ciangottini^{a,b}, L. Fanò^{a,b}, P. Lariccia^{a,b}, G. Mantovani^{a,b}, V. Mariani^{a,b}, M. Menichelli^a, F. Moscatelli^a, A. Piccinelli^{a,b}, A. Rossi^{a,b}, A. Santocchia^{a,b}, D. Spiga^a, T. Tedeschi^{a,b}

INFN Sezione di Pisa ^a, Università di Pisa ^b, Scuola Normale Superiore di Pisa ^c, Pisa Italy, Università di Siena ^d, Siena, Italy

P. Azzurri^a, G. Bagliesi^a, V. Bertacchi^{a,c}, L. Bianchini^a, T. Boccali^a, E. Bossini, R. Castaldi^a, M.A. Ciocci^{a,b}, R. Dell'Orso^a, M.R. Di Domenico^{a,d}, S. Donato^a, A. Giassi^a, M.T. Grippo^a, F. Ligabue^{a,c}, E. Manca^{a,c}, G. Mandorli^{a,c}, A. Messineo^{a,b}, F. Palla^a, G. Ramirez-Sanchez^{a,c}, A. Rizzi^{a,b}, G. Rolandi^{a,c}, S. Roy Chowdhury^{a,c}, A. Scribano^a, N. Shafiei^{a,b}, P. Spagnolo^a, R. Tenchini^a, G. Tonelli^{a,b}, N. Turini^{a,d}, A. Venturi^a, P.G. Verdini^a

INFN Sezione di Roma ^a, Sapienza Università di Roma ^b, Rome, Italy

F. Cavallari^a, M. Cipriani^{a,b}, D. Del Re^{a,b}, E. Di Marco^a, M. Diemoz^a, E. Longo^{a,b}, P. Meridiani^a, G. Organtini^{a,b}, F. Pandolfi^a, R. Paramatti^{a,b}, C. Quaranta^{a,b}, S. Rahatlou^{a,b}, C. Rovelli^a, F. Santanastasio^{a,b}, L. Soffi^{a,b}, R. Tramontano^{a,b}

INFN Sezione di Torino ^a, Università di Torino ^b, Torino, Italy, Università del Piemonte Orientale ^c, Novara, Italy

N. Amapane^{a,b}, R. Arcidiacono^{a,c}, S. Argiro^{a,b}, M. Arneodo^{a,c}, N. Bartosik^a, R. Bellan^{a,b}, A. Bellora^{a,b}, J. Berenguer Antequera^{a,b}, C. Biino^a, A. Cappati^{a,b}, N. Cartiglia^a, S. Cometti^a, M. Costa^{a,b}, R. Covarelli^{a,b}, N. Demaria^a, B. Kiani^{a,b}, F. Legger^a, C. Mariotti^a, S. Maselli^a, E. Migliore^{a,b}, V. Monaco^{a,b}, E. Monteil^{a,b}, M. Monteno^a, M.M. Obertino^{a,b}, G. Ortona^a, L. Pacher^{a,b}, N. Pastrone^a, M. Pelliccioni^a, G.L. Pinna Angioni^{a,b}, M. Ruspa^{a,c}, R. Salvatico^{a,b}, K. Shchelina^{a,b}, F. Siviero^{a,b}, V. Sola^a, A. Solano^{a,b}, D. Soldi^{a,b}, A. Staiano^a, M. Tornago^{a,b}, D. Trocino^{a,b}

INFN Sezione di Trieste ^a, Università di Trieste ^b, Trieste, Italy

S. Belforte^a, V. Candelise^{a,b}, M. Casarsa^a, F. Cossutti^a, A. Da Rold^{a,b}, G. Della Ricca^{a,b}, F. Vazzoler^{a,b}

Kyungpook National University, Daegu, Korea

S. Dogra, C. Huh, B. Kim, D.H. Kim, G.N. Kim, J. Lee, S.W. Lee, C.S. Moon, Y.D. Oh, S.I. Pak, B.C. Radburn-Smith, S. Sekmen, Y.C. Yang

Chonnam National University, Institute for Universe and Elementary Particles, Kwangju, Korea

H. Kim, D.H. Moon

Hanyang University, Seoul, Korea

T.J. Kim, J. Park

Korea University, Seoul, Korea

S. Cho, S. Choi, Y. Go, B. Hong, K. Lee, K.S. Lee, J. Lim, J. Park, S.K. Park, J. Yoo

Kyung Hee University, Department of Physics, Seoul, Republic of Korea

J. Goh, A. Gurtu

Sejong University, Seoul, Korea

H.S. Kim, Y. Kim

Seoul National University, Seoul, Korea

J. Almond, J.H. Bhyun, J. Choi, S. Jeon, J. Kim, J.S. Kim, S. Ko, H. Kwon, H. Lee, S. Lee, B.H. Oh, M. Oh, S.B. Oh, H. Seo, U.K. Yang, I. Yoon

University of Seoul, Seoul, Korea

D. Jeon, J.H. Kim, B. Ko, J.S.H. Lee, I.C. Park, Y. Roh, D. Song, I.J. Watson

Yonsei University, Department of Physics, Seoul, Korea

S. Ha, H.D. Yoo

Sungkyunkwan University, Suwon, Korea

Y. Choi, Y. Jeong, H. Lee, Y. Lee, I. Yu

College of Engineering and Technology, American University of the Middle East (AUM), Egaila, Kuwait

T. Beyrouthy, Y. Maghrbi

Riga Technical University, Riga, Latvia

V. Veckalns⁴⁵

Vilnius University, Vilnius, Lithuania

M. Ambrozys, A. Juodagalvis, A. Rinkevicius, G. Tamulaitis, A. Vaitkevicius

National Centre for Particle Physics, Universiti Malaya, Kuala Lumpur, Malaysia

W.A.T. Wan Abdullah, M.N. Yusli, Z. Zolkapli

Universidad de Sonora (UNISON), Hermosillo, Mexico

J.F. Benitez, A. Castaneda Hernandez, J.A. Murillo Quijada, L. Valencia Palomo

Centro de Investigacion y de Estudios Avanzados del IPN, Mexico City, Mexico

G. Ayala, H. Castilla-Valdez, E. De La Cruz-Burelo, I. Heredia-De La Cruz⁴⁶, R. Lopez-Fernandez, C.A. Mondragon Herrera, D.A. Perez Navarro, A. Sanchez-Hernandez

Universidad Iberoamericana, Mexico City, Mexico

S. Carrillo Moreno, C. Oropeza Barrera, M. Ramirez-Garcia, F. Vazquez Valencia

Benemerita Universidad Autonoma de Puebla, Puebla, Mexico

I. Pedraza, H.A. Salazar Ibarguen, C. Uribe Estrada

University of Montenegro, Podgorica, Montenegro

J. Mijuskovic⁴⁷, N. Raicevic

University of Auckland, Auckland, New Zealand

D. Krofcheck

University of Canterbury, Christchurch, New Zealand

S. Bheesette, P.H. Butler

National Centre for Physics, Quaid-I-Azam University, Islamabad, Pakistan

A. Ahmad, M.I. Asghar, A. Awais, M.I.M. Awan, H.R. Hoorani, W.A. Khan, M.A. Shah, M. Shoaib, M. Waqas

AGH University of Science and Technology Faculty of Computer Science, Electronics and Telecommunications, Krakow, Poland

V. Avati, L. Grzanka, M. Malawski

National Centre for Nuclear Research, Swierk, Poland

H. Bialkowska, M. Bluj, B. Boimska, T. Frueboes, M. Górski, M. Kazana, M. Szleper, P. Traczyk, P. Zalewski

Institute of Experimental Physics, Faculty of Physics, University of Warsaw, Warsaw, Poland

K. Bunkowski, K. Doroba, A. Kalinowski, M. Konecki, J. Krolikowski, M. Walczak

Laboratório de Instrumentação e Física Experimental de Partículas, Lisboa, Portugal

M. Araujo, P. Bargassa, D. Bastos, A. Boletti, P. Faccioli, M. Gallinaro, J. Hollar, N. Leonardo, T. Niknejad, J. Seixas, O. Toldaiev, J. Varela

Joint Institute for Nuclear Research, Dubna, Russia

S. Afanasiev, D. Budkouski, P. Bunin, M. Gavrilenko, I. Golutvin, I. Gorbunov, A. Kamenev, V. Karjavine, A. Lanev, A. Malakhov, V. Matveev^{48,49}, V. Palichik, V. Perelygin, M. Savina, D. Seitova, V. Shalaev, S. Shmatov, S. Shulha, V. Smirnov, O. Teryaev, N. Voytishin, A. Zarubin, I. Zhizhin

Petersburg Nuclear Physics Institute, Gatchina (St. Petersburg), Russia

G. Gavrilo, V. Golovtsov, Y. Ivanov, V. Kim⁵⁰, E. Kuznetsova⁵¹, V. Murzin, V. Oreshkin, I. Smirnov, D. Sosnov, V. Sulimov, L. Uvarov, S. Volkov, A. Vorobyev

Institute for Nuclear Research, Moscow, Russia

Yu. Andreev, A. Dermenev, S. Gninenko, N. Golubev, A. Karneyeu, M. Kirsanov, N. Krasnikov, A. Pashenkov, G. Pivovarov, D. Tlisov[†], A. Toropin

Institute for Theoretical and Experimental Physics named by A.I. Alikhanov of NRC 'Kurchatov Institute', Moscow, Russia

V. Epshteyn, V. Gavrilo, N. Lychkovskaya, A. Nikitenko⁵², V. Popov, G. Safronov, A. Spiridonov, A. Stepenov, M. Toms, E. Vlasov, A. Zhokin

Moscow Institute of Physics and Technology, Moscow, Russia

T. Aushev

National Research Nuclear University 'Moscow Engineering Physics Institute' (MEPhI), Moscow, Russia

R. Chistov⁵³, M. Danilov⁵⁴, A. Oskin, P. Parygin, S. Polikarpov⁵³

P.N. Lebedev Physical Institute, Moscow, Russia

V. Andreev, M. Azarkin, I. Dremin, M. Kirakosyan, A. Terkulov

Skobeltsyn Institute of Nuclear Physics, Lomonosov Moscow State University, Moscow, Russia

A. Belyaev, E. Boos, M. Dubinin⁵⁵, L. Dudko, A. Ershov, A. Gribushin, V. Klyukhin, O. Kodolova, I. Lokhtin, S. Obraztsov, S. Petrushanko, V. Savrin, A. Snigirev

Novosibirsk State University (NSU), Novosibirsk, Russia

V. Blinov⁵⁶, T. Dimova⁵⁶, L. Kardapoltsev⁵⁶, I. Ovtin⁵⁶, Y. Skovpen⁵⁶

Institute for High Energy Physics of National Research Centre 'Kurchatov Institute', Protvino, Russia

I. Azhgirey, I. Bayshev, V. Kachanov, A. Kalinin, D. Konstantinov, V. Petrov, R. Ryutin, A. Sobol, S. Troshin, N. Tyurin, A. Uzunian, A. Volkov

National Research Tomsk Polytechnic University, Tomsk, Russia

A. Babaev, V. Okhotnikov, L. Sukhikh

Tomsk State University, Tomsk, Russia

V. Borchsh, V. Ivanchenko, E. Tcherniaev

University of Belgrade: Faculty of Physics and VINCA Institute of Nuclear Sciences, Belgrade, Serbia

P. Adzic⁵⁷, M. Dordevic, P. Milenovic, J. Milosevic, V. Milosevic

Centro de Investigaciones Energéticas Medioambientales y Tecnológicas (CIEMAT), Madrid, Spain

M. Aguilar-Benitez, J. Alcaraz Maestre, A. Álvarez Fernández, I. Bachiller, M. Barrio Luna, Cristina F. Bedoya, C.A. Carrillo Montoya, M. Cepeda, M. Cerrada, N. Colino, B. De La Cruz, A. Delgado Peris, J.P. Fernández Ramos, J. Flix, M.C. Fouz, O. Gonzalez Lopez, S. Goy Lopez, J.M. Hernandez, M.I. Josa, J. León Holgado, D. Moran, Á. Navarro Tobar, A. Pérez-Calero Yzquierdo, J. Puerta Pelayo, I. Redondo, L. Romero, S. Sánchez Navas, M.S. Soares, L. Urda Gómez, C. Willmott

Universidad Autónoma de Madrid, Madrid, Spain

J.F. de Trocóniz, R. Reyes-Almanza

Universidad de Oviedo, Instituto Universitario de Ciencias y Tecnologías Espaciales de Asturias (ICTEA), Oviedo, Spain

B. Alvarez Gonzalez, J. Cuevas, C. Erice, J. Fernandez Menendez, S. Folgueras, I. Gonzalez Caballero, E. Palencia Cortezon, C. Ramón Álvarez, J. Ripoll Sau, V. Rodríguez Bouza, A. Trapote

Instituto de Física de Cantabria (IFCA), CSIC-Universidad de Cantabria, Santander, Spain

J.A. Brochero Cifuentes, I.J. Cabrillo, A. Calderon, B. Chazin Quero, J. Duarte Campderros, M. Fernandez, C. Fernandez Madrazo, P.J. Fernández Manteca, A. García Alonso, G. Gomez, C. Martinez Rivero, P. Martinez Ruiz del Arbol, F. Matorras, J. Piedra Gomez, C. Prieels, F. Ricci-Tam, T. Rodrigo, A. Ruiz-Jimeno, L. Scodellaro, N. Trevisani, I. Vila, J.M. Vizán García

University of Colombo, Colombo, Sri Lanka

MK Jayananda, B. Kailasapathy⁵⁸, D.U.J. Sonnadara, DDC Wickramarathna

University of Ruhuna, Department of Physics, Matara, Sri Lanka

W.G.D. Dharmaratna, K. Liyanage, N. Perera, N. Wickramage

CERN, European Organization for Nuclear Research, Geneva, Switzerland

T.K. Aarrestad, D. Abbaneo, J. Alimena, E. Auffray, G. Auzinger, J. Baechler, P. Baillon[†], A.H. Ball, D. Barney, J. Bendavid, N. Beni, M. Bianco, A. Bocci, E. Brondolin, T. Camporesi, M. Capeans Garrido, G. Cerminara, S.S. Chhibra, L. Cristella, D. d'Enterria, A. Dabrowski, N. Daci, A. David, A. De Roeck, M. Deile, R. Di Maria, M. Dobson, M. Dünser, N. Dupont, A. Elliott-Peisert, N. Emriskova, F. Fallavollita⁵⁹, D. Fasanella, S. Fiorendi, A. Florent, G. Franzoni, J. Fulcher, W. Funk, S. Giani, D. Gigi, K. Gill, F. Glege, L. Gouskos, M. Haranko, J. Hegeman, Y. Iiyama, V. Innocente, T. James, P. Janot, J. Kaspar, J. Kieseler, M. Komm, N. Kratochwil, C. Lange, S. Laurila, P. Lecoq, K. Long, C. Lourenço, L. Malgeri, S. Mallios, M. Mannelli, F. Meijers, S. Mersi, E. Meschi, F. Moortgat, M. Mulders, S. Orfanelli, L. Orsini, F. Pantaleo, L. Pape, E. Perez, M. Peruzzi, A. Petrilli, G. Petrucciani, A. Pfeiffer, M. Pierini, M. Pitt, H. Qu, T. Quast, D. Rabady, A. Racz, M. Rieger, M. Rovere, H. Sakulin, J. Salfeld-Nebgen, S. Scarfi, C. Schäfer, C. Schwick, M. Selvaggi, A. Sharma, P. Silva, W. Snoeys, P. Sphicas⁶⁰, S. Summers, V.R. Tavolaro, D. Treille, A. Tsirou, G.P. Van Onsem, M. Verzetti, K.A. Wozniak, W.D. Zeuner

Paul Scherrer Institut, Villigen, Switzerland

L. Caminada⁶¹, A. Ebrahimi, W. Erdmann, R. Horisberger, Q. Ingram, H.C. Kaestli, D. Kotlinski, U. Langenegger, M. Missiroli, T. Rohe

ETH Zurich - Institute for Particle Physics and Astrophysics (IPA), Zurich, Switzerland

K. Androsov⁶², M. Backhaus, P. Berger, A. Calandri, N. Chernyavskaya, A. De Cosa, G. Dissertori, M. Dittmar, M. Donegà, C. Dorfer, T. Gadek, T.A. Gómez Espinosa, C. Grab, D. Hits, W. Lustermann, A.-M. Lyon, R.A. Manzoni, C. Martin Perez, M.T. Meinhard,

F. Micheli, F. Nessi-Tedaldi, J. Niedziela, F. Pauss, V. Perovic, G. Perrin, S. Pigazzini, M.G. Ratti, M. Reichmann, C. Reissel, T. Reitenspiess, B. Ristic, D. Ruini, D.A. Sanz Becerra, M. Schönenberger, V. Stampf, J. Steggemann⁶², R. Wallny, D.H. Zhu

Universität Zürich, Zurich, Switzerland

C. Amsler⁶³, C. Botta, D. Brzhechko, M.F. Canelli, A. De Wit, R. Del Burgo, J.K. Heikkilä, M. Huwiler, A. Jofrehei, B. Kilminster, S. Leontsinis, A. Macchiolo, P. Meiring, V.M. Mikuni, U. Molinatti, I. Neutelings, G. Rauco, A. Reimers, P. Robmann, S. Sanchez Cruz, K. Schweiger, Y. Takahashi

National Central University, Chung-Li, Taiwan

C. Adloff⁶⁴, C.M. Kuo, W. Lin, A. Roy, T. Sarkar³⁶, S.S. Yu

National Taiwan University (NTU), Taipei, Taiwan

L. Ceard, P. Chang, Y. Chao, K.F. Chen, P.H. Chen, W.-S. Hou, Y.y. Li, R.-S. Lu, E. Paganis, A. Psallidas, A. Steen, E. Yazgan, P.r. Yu

Chulalongkorn University, Faculty of Science, Department of Physics, Bangkok, Thailand

B. Asavapibhop, C. Asawatangtrakuldee, N. Srimanobhas

Çukurova University, Physics Department, Science and Art Faculty, Adana, Turkey

M.N. Bakirci⁶⁵, F. Boran, S. Damarseckin⁶⁶, Z.S. Demiroglu, F. Dolek, I. Dumanoglu⁶⁷, G. Gokbulut, Y. Guler, E. Gurpinar Guler⁶⁸, I. Hos⁶⁹, C. Isik, E.E. Kangal⁷⁰, O. Kara, A. Kayis Topaksu, U. Kiminsu, G. Onengut, K. Ozdemir⁷¹, A.E. Simsek, B. Tali⁷², U.G. Tok, H. Topakli⁷³, S. Turkcapar, I.S. Zorbakir, C. Zorbilmez

Middle East Technical University, Physics Department, Ankara, Turkey

B. Isildak⁷⁴, G. Karapinar⁷⁵, K. Ocalan⁷⁶, M. Yalvac⁷⁷

Bogazici University, Istanbul, Turkey

B. Akgun, I.O. Atakisi, E. Gülmez, M. Kaya⁷⁸, O. Kaya⁷⁹, Ö. Özçelik, S. Tekten⁸⁰, E.A. Yetkin⁸¹

Istanbul Technical University, Istanbul, Turkey

A. Cakir, K. Cankocak⁶⁷, Y. Komurcu, S. Sen⁸²

Istanbul University, Istanbul, Turkey

F. Aydogmus Sen, S. Cerci⁷², B. Kaynak, S. Ozkorucuklu, D. Sunar Cerci⁷²

Institute for Scintillation Materials of National Academy of Science of Ukraine, Kharkov, Ukraine

B. Grynyov

National Scientific Center, Kharkov Institute of Physics and Technology, Kharkov, Ukraine

L. Levchuk

University of Bristol, Bristol, United Kingdom

E. Bhal, S. Bologna, J.J. Brooke, A. Bundock, E. Clement, D. Cussans, H. Flacher, J. Goldstein, G.P. Heath, H.F. Heath, L. Kreczko, B. Krikler, S. Paramesvaran, T. Sakuma, S. Seif El Nasr-Storey, V.J. Smith, N. Stylianou⁸³, J. Taylor, A. Titterton

Rutherford Appleton Laboratory, Didcot, United Kingdom

K.W. Bell, A. Belyaev⁸⁴, C. Brew, R.M. Brown, D.J.A. Cockerill, K.V. Ellis, K. Harder, S. Harper, J. Linacre, K. Manolopoulos, D.M. Newbold, E. Olaiya, D. Petyt, T. Reis, T. Schuh, C.H. Shepherd-Themistocleous, A. Thea, I.R. Tomalin, T. Williams

Imperial College, London, United Kingdom

R. Bainbridge, P. Bloch, S. Bonomally, J. Borg, S. Breeze, O. Buchmuller, V. Cepaitis, G.S. Chahal⁸⁵, D. Colling, P. Dauncey, G. Davies, M. Della Negra, S. Fayer, G. Fedi, G. Hall, M.H. Hassanshahi, G. Iles, J. Langford, L. Lyons, A.-M. Magnan, S. Malik, A. Martelli, J. Nash⁸⁶, V. Palladino, M. Pesaresi, D.M. Raymond, A. Richards, A. Rose, E. Scott, C. Seez, A. Shtipliyski, A. Tapper, K. Uchida, T. Virdee¹⁹, N. Wardle, S.N. Webb, D. Winterbottom, A.G. Zecchinelli

Brunel University, Uxbridge, United Kingdom

J.E. Cole, A. Khan, P. Kyberd, C.K. Mackay, I.D. Reid, L. Teodorescu, S. Zahid

Baylor University, Waco, USA

S. Abdullin, A. Brinkerhoff, B. Caraway, J. Dittmann, K. Hatakeyama, A.R. Kanuganti, B. McMaster, N. Pastika, S. Sawant, C. Smith, C. Sutantawibul, J. Wilson

Catholic University of America, Washington, DC, USA

R. Bartek, A. Dominguez, R. Uniyal, A.M. Vargas Hernandez

The University of Alabama, Tuscaloosa, USA

A. Buccilli, O. Charaf, S.I. Cooper, D. Di Croce, S.V. Gleyzer, C. Henderson, C.U. Perez, P. Rumerio, C. West

Boston University, Boston, USA

A. Akpinar, A. Albert, D. Arcaro, C. Cosby, Z. Demiragli, D. Gastler, J. Rohlf, K. Salyer, D. Sperka, D. Spitzbart, I. Suarez, S. Yuan, D. Zou

Brown University, Providence, USA

G. Benelli, B. Burkle, X. Coubez²⁰, D. Cutts, Y.t. Duh, M. Hadley, U. Heintz, J.M. Hogan⁸⁷, K.H.M. Kwok, E. Laird, G. Landsberg, K.T. Lau, J. Lee, J. Luo, M. Narain, S. Sagir⁸⁸, E. Usai, W.Y. Wong, X. Yan, D. Yu, W. Zhang

University of California, Davis, Davis, USA

C. Brainerd, R. Breedon, M. Calderon De La Barca Sanchez, M. Chertok, J. Conway, P.T. Cox, R. Erbacher, F. Jensen, O. Kukral, R. Lander, M. Mulhearn, D. Pellett, D. Taylor, M. Tripathi, Y. Yao, F. Zhang

University of California, Los Angeles, USA

M. Bachtis, R. Cousins, A. Dasgupta, A. Datta, D. Hamilton, J. Hauser, M. Ignatenko, M.A. Iqbal, T. Lam, N. Mccoll, W.A. Nash, S. Regnard, D. Saltzberg, C. Schnaible, B. Stone, V. Valuev

University of California, Riverside, Riverside, USA

K. Burt, Y. Chen, R. Clare, J.W. Gary, G. Hanson, G. Karapostoli, O.R. Long, N. Manganelli, M. Olmedo Negrete, W. Si, S. Wimpenny, Y. Zhang

University of California, San Diego, La Jolla, USA

J.G. Branson, P. Chang, S. Cittolin, S. Cooperstein, N. Deelen, J. Duarte, R. Gerosa, L. Giannini, D. Gilbert, J. Guiang, R. Kansal, V. Krutelyov, R. Lee, J. Letts, M. Masciovecchio, S. May, S. Padhi, M. Pieri, B.V. Sathia Narayanan, V. Sharma, M. Tadel, A. Vartak, F. Würthwein, Y. Xiang, A. Yagil

University of California, Santa Barbara - Department of Physics, Santa Barbara, USA

N. Amin, C. Campagnari, M. Citron, A. Dorsett, V. Dutta, J. Incandela, M. Kilpatrick, B. Marsh, H. Mei, A. Ovcharova, M. Quinnan, J. Richman, U. Sarica, D. Stuart, S. Wang

California Institute of Technology, Pasadena, USA

A. Bornheim, O. Cerri, I. Dutta, J.M. Lawhorn, N. Lu, J. Mao, H.B. Newman, J. Ngadiuba, T.Q. Nguyen, M. Spiropulu, J.R. Vlimant, C. Wang, S. Xie, Z. Zhang, R.Y. Zhu

Carnegie Mellon University, Pittsburgh, USA

J. Alison, M.B. Andrews, T. Ferguson, T. Mudholkar, M. Paulini, I. Vorobiev

University of Colorado Boulder, Boulder, USA

J.P. Cumalat, W.T. Ford, E. MacDonald, R. Patel, A. Perloff, K. Stenson, K.A. Ulmer, S.R. Wagner

Cornell University, Ithaca, USA

J. Alexander, Y. Cheng, J. Chu, D.J. Cranshaw, K. Mcdermott, J. Monroy, J.R. Patterson, D. Quach, A. Ryd, W. Sun, S.M. Tan, Z. Tao, J. Thom, P. Wittich, M. Zientek

Fermi National Accelerator Laboratory, Batavia, USA

M. Albrow, M. Alyari, G. Apollinari, A. Apresyan, A. Apyan, S. Banerjee, L.A.T. Bauerdick, A. Beretvas, D. Berry, J. Berryhill, P.C. Bhat, K. Burkett, J.N. Butler, A. Canepa, G.B. Cerati, H.W.K. Cheung, F. Chlebana, M. Cremonesi, K.F. Di Petrillo, V.D. Elvira, J. Freeman, Z. Gecse, L. Gray, D. Green, S. Grünendahl, O. Gutsche, R.M. Harris, R. Heller, T.C. Herwig, J. Hirschauer, B. Jayatilaka, S. Jindariani, M. Johnson, U. Joshi, P. Klabbers, T. Klijnsma, B. Klima, M.J. Kortelainen, S. Lammel, D. Lincoln, R. Lipton, T. Liu, J. Lykken, C. Madrid, K. Maeshima, C. Mantilla, D. Mason, P. McBride, P. Merkel, S. Mrenna, S. Nahn, V. O'Dell, V. Papadimitriou, K. Pedro, C. Pena⁵⁵, O. Prokofyev, F. Ravera, A. Reinsvold Hall, L. Ristori, B. Schneider, E. Sexton-Kennedy, N. Smith, A. Soha, L. Spiegel, S. Stoynev, J. Strait, L. Taylor, S. Tkaczyk, N.V. Tran, L. Uplegger, E.W. Vaandering, H.A. Weber, A. Woodard

University of Florida, Gainesville, USA

D. Acosta, P. Avery, D. Bourilkov, L. Cadamuro, V. Cherepanov, F. Errico, R.D. Field, D. Guerrero, B.M. Joshi, M. Kim, J. Konigsberg, A. Korytov, K.H. Lo, K. Matchev, N. Menendez, G. Mitselmakher, D. Rosenzweig, K. Shi, J. Sturdy, J. Wang, E. Yigitbasi, X. Zuo

Florida State University, Tallahassee, USA

T. Adams, A. Askew, D. Diaz, R. Habibullah, S. Hagopian, V. Hagopian, K.F. Johnson, R. Khurana, T. Kolberg, G. Martinez, H. Prosper, C. Schiber, R. Yohay, J. Zhang

Florida Institute of Technology, Melbourne, USA

M.M. Baarmand, S. Butalla, T. Elkafrawy¹³, M. Hohlmann, R. Kumar Verma, D. Noonan, M. Rahmani, M. Saunders, F. Yumiceva

University of Illinois at Chicago (UIC), Chicago, USA

M.R. Adams, L. Apanasevich, H. Becerril Gonzalez, R. Cavanaugh, X. Chen, S. Dittmer, O. Evdokimov, C.E. Gerber, D.A. Hangal, D.J. Hofman, C. Mills, G. Oh, T. Roy, M.B. Tonjes, N. Varelas, J. Viinikainen, X. Wang, Z. Wu, Z. Ye

The University of Iowa, Iowa City, USA

M. Alhousseini, K. Dilsiz⁸⁹, S. Durgut, R.P. Gandrajula, M. Haytmyradov, V. Khristenko, O.K. Köseyan, J.-P. Merlo, A. Mestvirishvili⁹⁰, A. Moeller, J. Nachtman, H. Ogul⁹¹, Y. Onel, F. Ozok⁹², A. Penzo, C. Snyder, E. Tiras⁹³, J. Wetzel

Johns Hopkins University, Baltimore, USA

O. Amram, B. Blumenfeld, L. Corcodilos, M. Eminizer, A.V. Gritsan, S. Kyriacou, P. Maksimovic, J. Roskes, M. Swartz, T.Á. Vámi

The University of Kansas, Lawrence, USA

C. Baldenegro Barrera, P. Baringer, A. Bean, A. Bylinkin, T. Isidori, S. Khalil, J. King,

G. Krintiras, A. Kropivnitskaya, C. Lindsey, N. Minafra, M. Murray, C. Rogan, C. Royon, S. Sanders, E. Schmitz, J.D. Tapia Takaki, Q. Wang, J. Williams, G. Wilson

Kansas State University, Manhattan, USA

S. Duric, A. Ivanov, K. Kaadze, D. Kim, Y. Maravin, T. Mitchell, A. Modak, K. Nam

Lawrence Livermore National Laboratory, Livermore, USA

F. Rebassoo, D. Wright

University of Maryland, College Park, USA

E. Adams, A. Baden, O. Baron, A. Belloni, S.C. Eno, Y. Feng, N.J. Hadley, S. Jabeen, R.G. Kellogg, T. Koeth, A.C. Mignerey, S. Nabili, M. Seidel, A. Skuja, S.C. Tonwar, L. Wang, K. Wong

Massachusetts Institute of Technology, Cambridge, USA

D. Abercrombie, G. Andreassi, R. Bi, S. Brandt, W. Busza, I.A. Cali, Y. Chen, M. D'Alfonso, G. Gomez Ceballos, M. Goncharov, P. Harris, M. Hu, M. Klute, D. Kovalskyi, J. Krupa, Y.-J. Lee, B. Maier, A.C. Marini, C. Mironov, C. Paus, D. Rankin, C. Roland, G. Roland, Z. Shi, G.S.F. Stephans, K. Tatar, J. Wang, Z. Wang, B. Wyslouch

University of Minnesota, Minneapolis, USA

R.M. Chatterjee, A. Evans, P. Hansen, J. Hiltbrand, Sh. Jain, M. Krohn, Y. Kubota, Z. Lesko, J. Mans, M. Revering, R. Rusack, R. Saradhy, N. Schroeder, N. Strobbe, M.A. Wadud

University of Mississippi, Oxford, USA

J.G. Acosta, S. Oliveros

University of Nebraska-Lincoln, Lincoln, USA

K. Bloom, M. Bryson, S. Chauhan, D.R. Claes, C. Fangmeier, L. Finco, F. Golf, J.R. González Fernández, C. Joo, I. Kravchenko, J.E. Siado, G.R. Snow[†], W. Tabb, F. Yan

State University of New York at Buffalo, Buffalo, USA

G. Agarwal, H. Bandyopadhyay, L. Hay, I. Iashvili, A. Kharchilava, C. McLean, D. Nguyen, J. Pekkanen, S. Rappoccio, A. Williams

Northeastern University, Boston, USA

G. Alverson, E. Barberis, C. Freer, Y. Haddad, A. Hortiangtham, J. Li, G. Madigan, B. Marzocchi, D.M. Morse, V. Nguyen, T. Orimoto, A. Parker, L. Skinnari, A. Tishelman-Charny, T. Wamorkar, B. Wang, A. Wisecarver, D. Wood

Northwestern University, Evanston, USA

S. Bhattacharya, J. Bueghly, Z. Chen, A. Gilbert, T. Gunter, K.A. Hahn, N. Odell, M.H. Schmitt, K. Sung, M. Velasco

University of Notre Dame, Notre Dame, USA

R. Band, R. Bucci, N. Dev, R. Goldouzian, M. Hildreth, K. Hurtado Anampa, C. Jessop, K. Lannon, N. Loukas, N. Marinelli, I. Mcalister, F. Meng, K. Mohrman, Y. Musienko⁴⁸, R. Ruchti, P. Siddireddy, M. Wayne, A. Wightman, M. Wolf, M. Zarucki, L. Zygala

The Ohio State University, Columbus, USA

B. Bylsma, B. Cardwell, L.S. Durkin, B. Francis, C. Hill, A. Lefeld, B.L. Winer, B.R. Yates

Princeton University, Princeton, USA

F.M. Addesa, B. Bonham, P. Das, G. Dezoort, P. Elmer, A. Frankenthal, B. Greenberg, N. Haubrich, S. Higginbotham, A. Kalogeropoulos, G. Kopp, S. Kwan, D. Lange, M.T. Lucchini, D. Marlow, K. Mei, I. Ojalvo, J. Olsen, C. Palmer, D. Stickland, C. Tully

University of Puerto Rico, Mayaguez, USA

S. Malik, S. Norberg

Purdue University, West Lafayette, USA

A.S. Bakshi, V.E. Barnes, R. Chawla, S. Das, L. Gutay, M. Jones, A.W. Jung, S. Karmarkar, M. Liu, G. Negro, N. Neumeister, G. Paspalaki, C.C. Peng, S. Piperov, A. Purohit, J.F. Schulte, M. Stojanovic¹⁶, J. Thieman, F. Wang, R. Xiao, W. Xie

Purdue University Northwest, Hammond, USA

J. Dolen, N. Parashar

Rice University, Houston, USA

A. Baty, S. Dildick, K.M. Ecklund, S. Freed, F.J.M. Geurts, A. Kumar, W. Li, B.P. Padley, R. Redjimi, J. Roberts[†], W. Shi, A.G. Stahl Leitton

University of Rochester, Rochester, USA

A. Bodek, P. de Barbaro, R. Demina, J.L. Dulemba, C. Fallon, T. Ferbel, M. Galanti, A. Garcia-Bellido, O. Hindrichs, A. Khukhunaishvili, E. Ranken, R. Taus

Rutgers, The State University of New Jersey, Piscataway, USA

B. Chiarito, J.P. Chou, A. Gandrakota, Y. Gershtein, E. Halkiadakis, A. Hart, M. Heindl, E. Hughes, S. Kaplan, O. Karacheban²³, I. Laflotte, A. Lath, R. Montalvo, K. Nash, M. Osherson, S. Salur, S. Schnetzer, S. Somalwar, R. Stone, S.A. Thayil, S. Thomas, H. Wang

University of Tennessee, Knoxville, USA

H. Acharya, A.G. Delannoy, S. Spanier

Texas A&M University, College Station, USA

O. Bouhali⁹⁴, M. Dalchenko, A. Delgado, R. Eusebi, J. Gilmore, T. Huang, T. Kamon⁹⁵, H. Kim, S. Luo, S. Malhotra, R. Mueller, D. Overton, D. Rathjens, A. Safonov

Texas Tech University, Lubbock, USA

N. Akchurin, J. Damgov, V. Hegde, S. Kunori, K. Lamichhane, S.W. Lee, T. Mengke, S. Muthumuni, T. Peltola, S. Undleeb, I. Volobouev, Z. Wang, A. Whitbeck

Vanderbilt University, Nashville, USA

E. Appelt, S. Greene, A. Gurrola, W. Johns, C. Maguire, A. Melo, H. Ni, K. Padeken, F. Romeo, P. Sheldon, S. Tuo, J. Velkovska

University of Virginia, Charlottesville, USA

M.W. Arenton, B. Cox, G. Cummings, J. Hakala, R. Hirosky, M. Joyce, A. Ledovskoy, A. Li, C. Neu, B. Tannenwald, E. Wolfe

Wayne State University, Detroit, USA

P.E. Karchin, N. Poudyal, P. Thapa

University of Wisconsin - Madison, Madison, WI, USA

K. Black, T. Bose, J. Buchanan, C. Caillol, S. Dasu, I. De Bruyn, P. Everaerts, F. Fienga, C. Galloni, H. He, M. Herndon, A. Hervé, U. Hussain, A. Lanaro, A. Loeliger, R. Loveless, J. Madhusudanan Sreekala, A. Mallampalli, A. Mohammadi, D. Pinna, A. Savin, V. Shang, V. Sharma, W.H. Smith, D. Teague, S. Trembath-reichert, W. Vetens

†: Deceased

1: Also at Vienna University of Technology, Vienna, Austria

2: Also at Institute of Basic and Applied Sciences, Faculty of Engineering, Arab Academy for Science, Technology and Maritime Transport, Alexandria, Egypt, Alexandria, Egypt

- 3: Also at Université Libre de Bruxelles, Bruxelles, Belgium
- 4: Also at Universidade Estadual de Campinas, Campinas, Brazil
- 5: Also at Federal University of Rio Grande do Sul, Porto Alegre, Brazil
- 6: Also at University of Chinese Academy of Sciences, Beijing, China
- 7: Also at Department of Physics, Tsinghua University, Beijing, China, Beijing, China
- 8: Also at UFMS, Nova Andradina, Brazil
- 9: Also at Nanjing Normal University Department of Physics, Nanjing, China
- 10: Now at The University of Iowa, Iowa City, USA
- 11: Also at Institute for Theoretical and Experimental Physics named by A.I. Alikhanov of NRC 'Kurchatov Institute', Moscow, Russia
- 12: Also at Joint Institute for Nuclear Research, Dubna, Russia
- 13: Also at Ain Shams University, Cairo, Egypt
- 14: Also at Zewail City of Science and Technology, Zewail, Egypt
- 15: Also at British University in Egypt, Cairo, Egypt
- 16: Also at Purdue University, West Lafayette, USA
- 17: Also at Université de Haute Alsace, Mulhouse, France
- 18: Also at Erzincan Binali Yildirim University, Erzincan, Turkey
- 19: Also at CERN, European Organization for Nuclear Research, Geneva, Switzerland
- 20: Also at RWTH Aachen University, III. Physikalisches Institut A, Aachen, Germany
- 21: Also at University of Hamburg, Hamburg, Germany
- 22: Also at Department of Physics, Isfahan University of Technology, Isfahan, Iran, Isfahan, Iran
- 23: Also at Brandenburg University of Technology, Cottbus, Germany
- 24: Also at Skobeltsyn Institute of Nuclear Physics, Lomonosov Moscow State University, Moscow, Russia
- 25: Also at Physics Department, Faculty of Science, Assiut University, Assiut, Egypt
- 26: Also at Eszterhazy Karoly University, Karoly Robert Campus, Gyongyos, Hungary
- 27: Also at Institute of Physics, University of Debrecen, Debrecen, Hungary, Debrecen, Hungary
- 28: Also at Institute of Nuclear Research ATOMKI, Debrecen, Hungary
- 29: Also at MTA-ELTE Lendület CMS Particle and Nuclear Physics Group, Eötvös Loránd University, Budapest, Hungary, Budapest, Hungary
- 30: Also at Wigner Research Centre for Physics, Budapest, Hungary
- 31: Also at IIT Bhubaneswar, Bhubaneswar, India, Bhubaneswar, India
- 32: Also at Institute of Physics, Bhubaneswar, India
- 33: Also at G.H.G. Khalsa College, Punjab, India
- 34: Also at Shoolini University, Solan, India
- 35: Also at University of Hyderabad, Hyderabad, India
- 36: Also at University of Visva-Bharati, Santiniketan, India
- 37: Also at Indian Institute of Technology (IIT), Mumbai, India
- 38: Also at Deutsches Elektronen-Synchrotron, Hamburg, Germany
- 39: Also at Sharif University of Technology, Tehran, Iran
- 40: Also at Department of Physics, University of Science and Technology of Mazandaran, Behshahr, Iran
- 41: Now at INFN Sezione di Bari ^a, Università di Bari ^b, Politecnico di Bari ^c, Bari, Italy
- 42: Also at Italian National Agency for New Technologies, Energy and Sustainable Economic Development, Bologna, Italy
- 43: Also at Centro Siciliano di Fisica Nucleare e di Struttura Della Materia, Catania, Italy
- 44: Also at Università di Napoli 'Federico II', NAPOLI, Italy

-
- 45: Also at Riga Technical University, Riga, Latvia, Riga, Latvia
 - 46: Also at Consejo Nacional de Ciencia y Tecnología, Mexico City, Mexico
 - 47: Also at IRFU, CEA, Université Paris-Saclay, Gif-sur-Yvette, France
 - 48: Also at Institute for Nuclear Research, Moscow, Russia
 - 49: Now at National Research Nuclear University 'Moscow Engineering Physics Institute' (MEPhI), Moscow, Russia
 - 50: Also at St. Petersburg State Polytechnical University, St. Petersburg, Russia
 - 51: Also at University of Florida, Gainesville, USA
 - 52: Also at Imperial College, London, United Kingdom
 - 53: Also at P.N. Lebedev Physical Institute, Moscow, Russia
 - 54: Also at Moscow Institute of Physics and Technology, Moscow, Russia, Moscow, Russia
 - 55: Also at California Institute of Technology, Pasadena, USA
 - 56: Also at Budker Institute of Nuclear Physics, Novosibirsk, Russia
 - 57: Also at Faculty of Physics, University of Belgrade, Belgrade, Serbia
 - 58: Also at Trincomalee Campus, Eastern University, Sri Lanka, Nilaveli, Sri Lanka
 - 59: Also at INFN Sezione di Pavia ^a, Università di Pavia ^b, Pavia, Italy, Pavia, Italy
 - 60: Also at National and Kapodistrian University of Athens, Athens, Greece
 - 61: Also at Universität Zürich, Zurich, Switzerland
 - 62: Also at Ecole Polytechnique Fédérale Lausanne, Lausanne, Switzerland
 - 63: Also at Stefan Meyer Institute for Subatomic Physics, Vienna, Austria, Vienna, Austria
 - 64: Also at Laboratoire d'Annecy-le-Vieux de Physique des Particules, IN2P3-CNRS, Annecy-le-Vieux, France
 - 65: Also at Gaziosmanpasa University, Tokat, Turkey
 - 66: Also at Şırnak University, Sirnak, Turkey
 - 67: Also at Near East University, Research Center of Experimental Health Science, Nicosia, Turkey
 - 68: Also at Konya Technical University, Konya, Turkey
 - 69: Also at Istanbul University - Cerrahpaşa, Faculty of Engineering, Istanbul, Turkey
 - 70: Also at Mersin University, Mersin, Turkey
 - 71: Also at Piri Reis University, Istanbul, Turkey
 - 72: Also at Adiyaman University, Adiyaman, Turkey
 - 73: Also at Tarsus University, MERSIN, Turkey
 - 74: Also at Ozyegin University, Istanbul, Turkey
 - 75: Also at Izmir Institute of Technology, Izmir, Turkey
 - 76: Also at Necmettin Erbakan University, Konya, Turkey
 - 77: Also at Bozok Universitetesi Rektörlüğü, Yozgat, Turkey, Yozgat, Turkey
 - 78: Also at Marmara University, Istanbul, Turkey
 - 79: Also at Milli Savunma University, Istanbul, Turkey
 - 80: Also at Kafkas University, Kars, Turkey
 - 81: Also at Istanbul Bilgi University, Istanbul, Turkey
 - 82: Also at Hacettepe University, Ankara, Turkey
 - 83: Also at Vrije Universiteit Brussel, Brussel, Belgium
 - 84: Also at School of Physics and Astronomy, University of Southampton, Southampton, United Kingdom
 - 85: Also at IPPP Durham University, Durham, United Kingdom
 - 86: Also at Monash University, Faculty of Science, Clayton, Australia
 - 87: Also at Bethel University, St. Paul, Minneapolis, USA, St. Paul, USA
 - 88: Also at Karamanoğlu Mehmetbey University, Karaman, Turkey
 - 89: Also at Bingöl University, Bingöl, Turkey

90: Also at Georgian Technical University, Tbilisi, Georgia

91: Also at Sinop University, Sinop, Turkey

92: Also at Mimar Sinan University, Istanbul, Istanbul, Turkey

93: Also at Erciyes University, KAYSERI, Turkey

94: Also at Texas A&M University at Qatar, Doha, Qatar

95: Also at Kyungpook National University, Daegu, Korea, Daegu, Korea